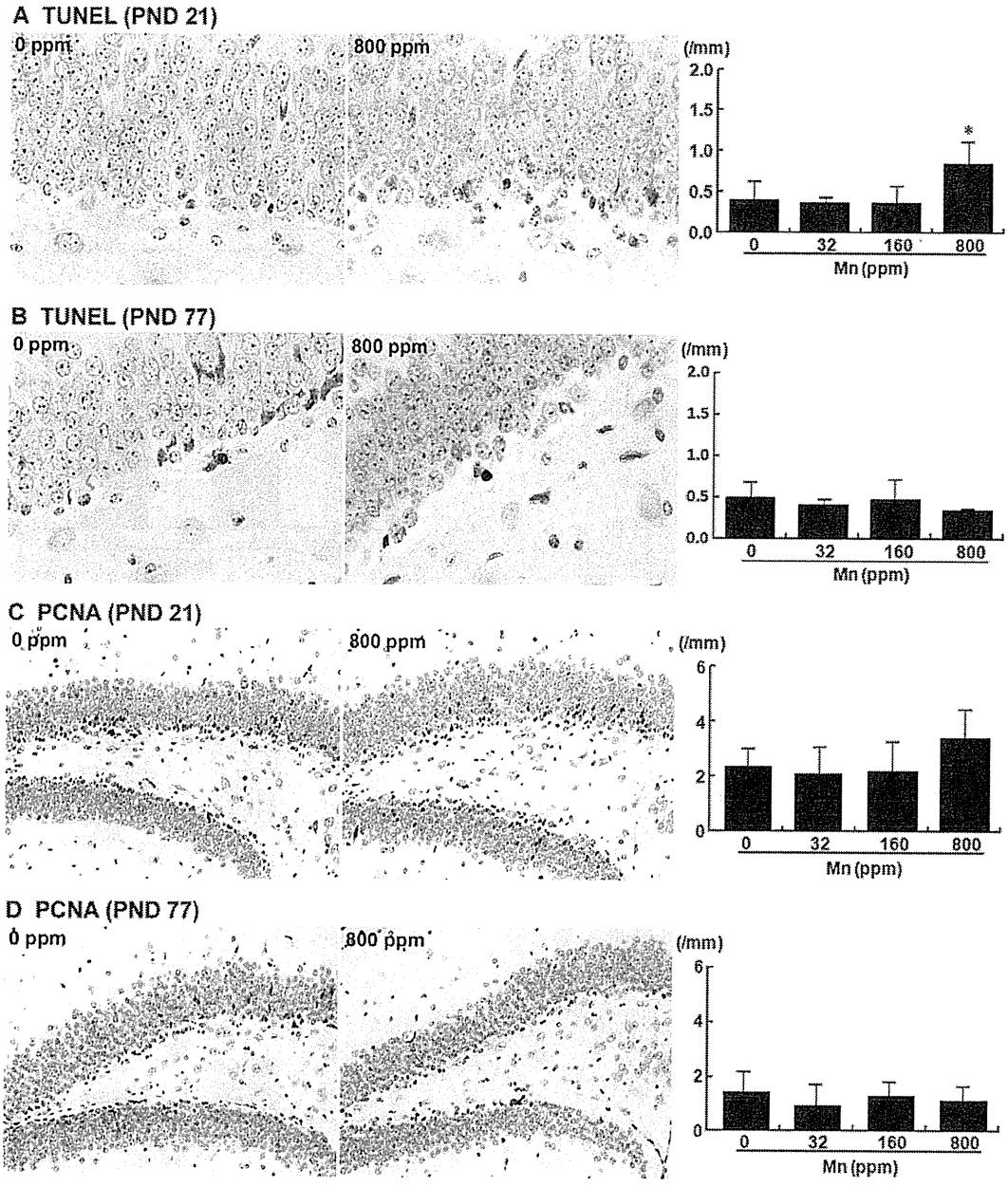

FIG. 6. Distribution of apoptotic cells and proliferating cells in the dentate SGZ of male offspring at both PNDs 21 and 77 exposed maternally to $MnCl_2$ from GD 10 to PND 21. (A) and (B) TUNEL-positive apoptotic cells at PNDs 21 and 77. (C) and (D) PCNA-positive cells at PNDs 21 and 77. Representative images from 0 ppm group (left) and from 800 ppm group (right) at PNDs 21 and 77. (A) and (B) Magnification, 400×. (C) and (D) Magnification, 200×. Graphs show the number of immunoreactive cells/unit length (mm) of the SGZ of bilateral hemispheres at PNDs 21 and 77. Values are expressed as the mean + SD. *Significantly different from the untreated controls by Dunnett's test or Steel's test ($p < 0.05$). For full color figures, please see online version.

1997). Also, it has been suggested that GABAergic interneurons in the hilar region release reelin and regulate the migration and maturation of newborn granule cells in adults (Lussier *et al.*, 2009). Interestingly, faint expression of mature neuronal markers, such as NeuN and microtubule-associated protein-2, has been reported to reflect the immature nature of neurons (Seki, 2002). An increase of GAD67-expressing cells at PND 21 after maternal $MnCl_2$ exposure was found in the present study, confirming the increase of GABAergic interneurons (Saegusa *et al.*, 2010). Therefore, the sustained increase of reelin-expressing and NeuN-lacking or weakly expressing neurons were considered immature GABAergic interneurons

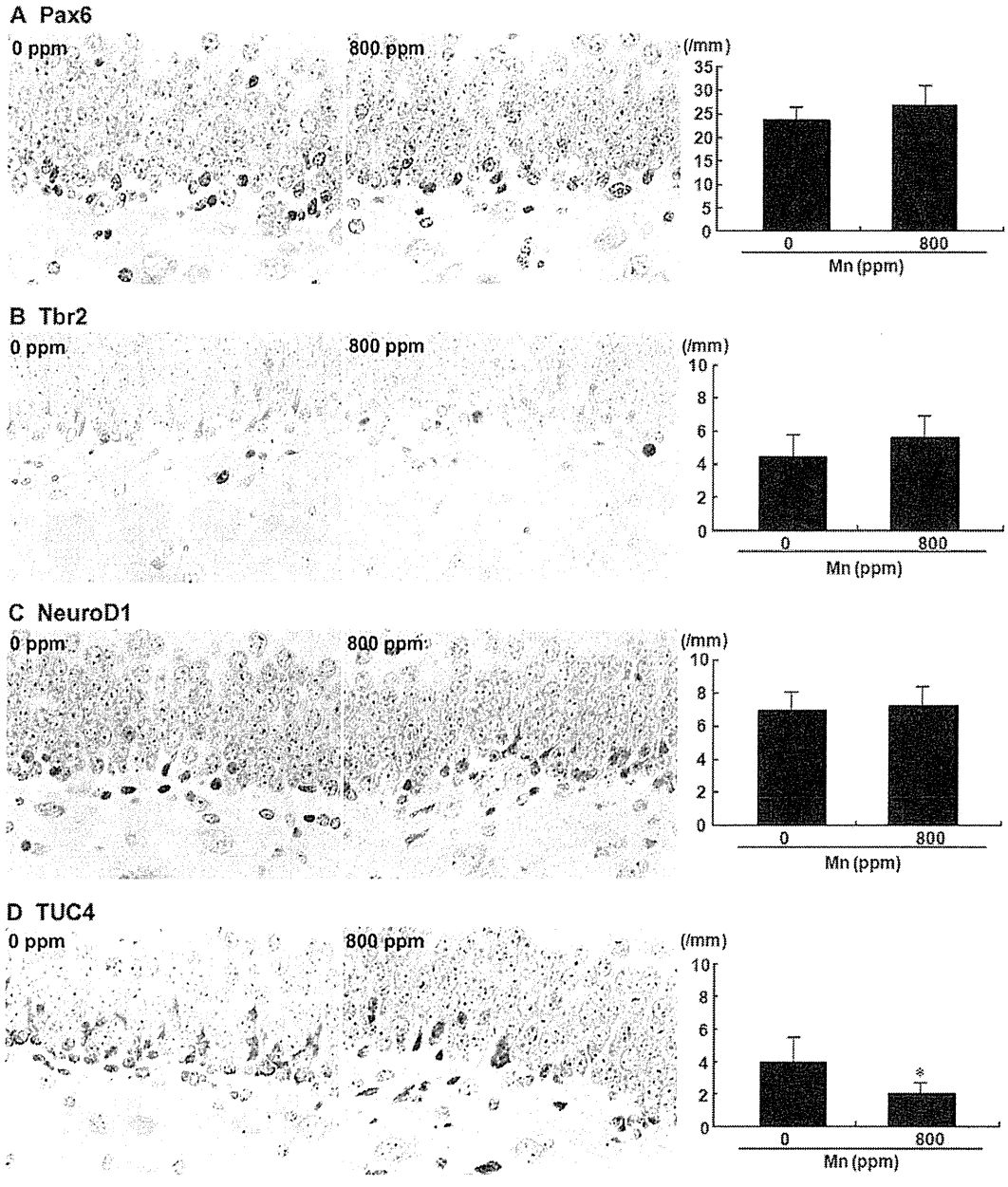

FIG. 7. Distribution of immunoreactive cells for Pax6, Tbr2, NeuroD1, and TUC4 in the dentate SGZ of male offspring at PND 21 exposed maternally to $MnCl_2$ from GD 10 to PND 21. (A) Pax6. (B) Tbr2. (C) NeuroD1. (D) TUC4. Representative images from 0 ppm group (left) and from 800 ppm group (right) at PND 21. Magnification, 400×. Graphs show the number of immunoreactive cells for each antigen/unit length (mm) of the SGZ of bilateral hemispheres at PND 21. Values are expressed as the mean + SD. * Significantly different from the untreated controls by Student's or Aspin-Welch's *t*-test ($p < 0.05$). For full color figures, please see online version.

responding to neuronal mismigration due to impaired neurogenesis of dentate granule cells even at the adult stage. A decrease of TUC4-expressing immature granule cells at PND 21 may be responsible for the initial increase of immature reelin-expressing interneurons in the hilus. The sustained increase of this population of cells may be a sign of continued aberration in neurogenesis and migration that causes the overproduction of immature granule cells at the adult stage. On the other hand, it has been reported that GABAergic interneurons provide direct neural inputs toward type 2 progenitor cells in the SGZ and promote neural differentiation (Tozuka *et al.*, 2005). Thus, sustained increases of NeuN-expressing neuron populations in the hilus with 800 ppm Mn through to the adult stage may represent mature interneurons that stop producing reelin but

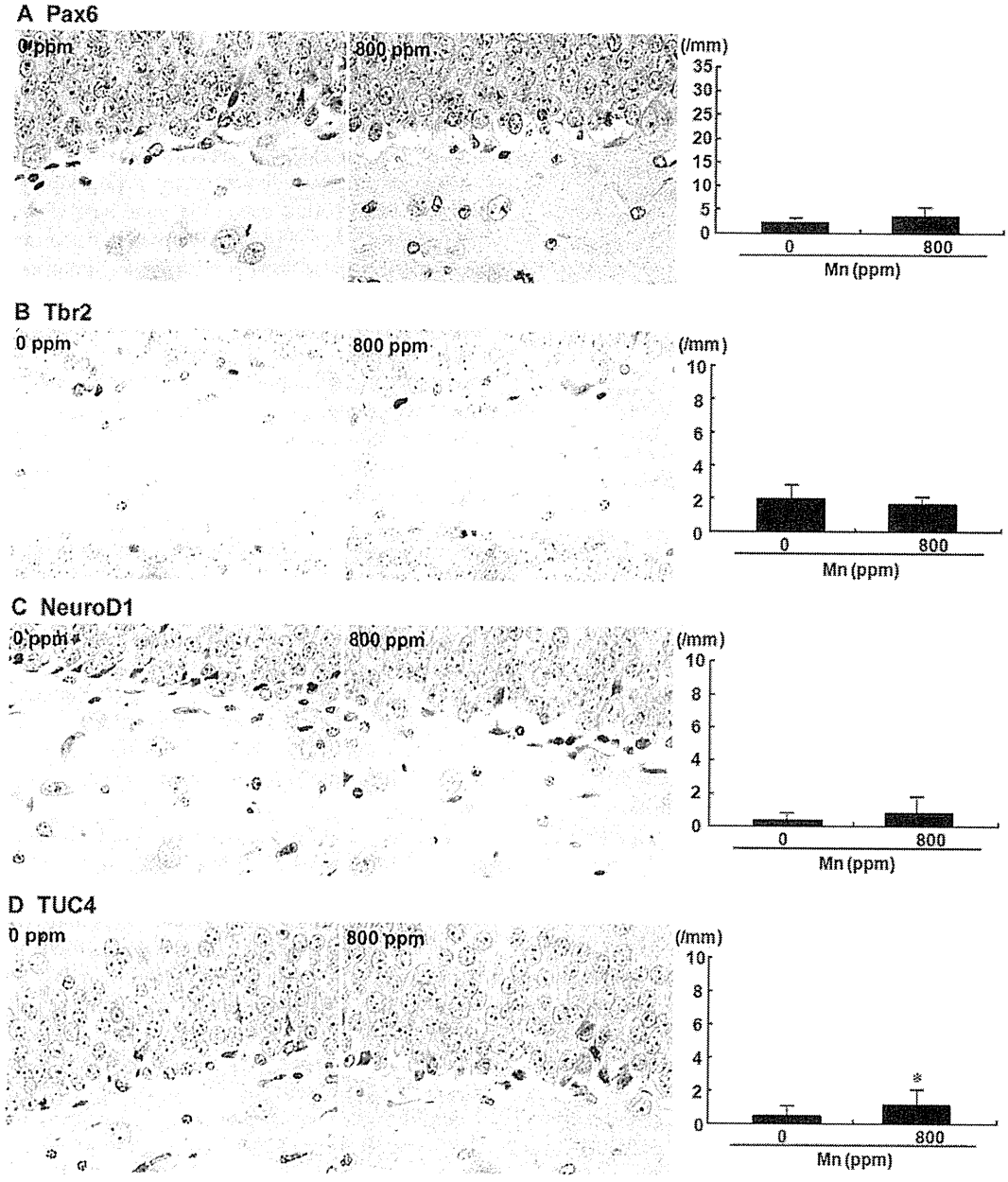

FIG. 8. Distribution of immunoreactive cells for Pax6, Tbr2, NeuroD1, and TUC4 in the dentate SGZ of male offspring at PND 77 exposed maternally to $MnCl_2$ from GD 10 to PND 21. (A) Pax6. (B) Tbr2. (C) NeuroD1. (D) TUC4. Representative images from 0 ppm group (left) and from 800 ppm group (right) at PND 77. Magnification, 400×. Graphs show the number of immunoreactive cells for each antigen/unit length (mm) of the SGZ of bilateral hemispheres at PND 77. Values are expressed as the mean + SD. * Significantly different from the untreated controls by Student's or Aspin-Welch's *t*-test ($p < 0.05$). For full color figures, please see online version.

facilitate progenitor cells to undergo differentiation to immature granule cells.

In the present study, we found systemic growth retardation in offspring after weaning following treatment with ≥ 160 ppm Mn, but we did not detect alterations in absolute brain weights in any $MnCl_2$-exposed groups as compared with untreated controls. In our previous study, maternal protein restriction causing progressive systematic growth retardation involving decreased brain weight did not affect neurogenesis and the distribution of GABAergic interneurons expressing reelin in offspring (Ohishi *et al.*, 2010). Therefore, we judge that Mn-induced systemic growth retardation observed here was weaker

TABLE 4
Real-Time RT-PCR Analysis in the Hippocampal Dentate Gyrus on PND 21

	0 ppm Mn		800 ppm Mn	
	Relative Transcript Level Normalized To		Relative Transcript Level Normalized To	
	Hprt	*Gapdh*	*Hprt*	*Gapdh*
Reln	1.02 ± 0.23[a]	1.23 ± 0.75	2.76 ± 0.35**	4.09 ± 0.97**
Lrp8	1.01 ± 0.14	1.08 ± 0.47	1.63 ± 0.29**	2.41 ± 0.39**
Vldlr	1.00 ± 0.05	1.10 ± 0.52	0.93 ± 0.09	1.38 ± 0.10
Gad1	1.00 ± 0.04	1.13 ± 0.58	1.86 ± 0.06**	2.76 ± 0.45**
Pax6	1.05 ± 0.40	1.03 ± 0.26	1.13 ± 0.40	1.66 ± 0.54
Eomes	1.06 ± 0.47	1.02 ± 0.21	1.22 ± 0.48	1.80 ± 0.66
Dpysl3	1.00 ± 0.06	1.12 ± 0.06	0.47 ± 0.04**	0.69 ± 0.03**

Notes. *Hprt*, hypoxanthine-guanine phosphoribosyltransferase; *Gapdh*, glyceraldehyde 3-phosphate dehydrogenase; *Reln*, reelin; *Lrp8*, low density lipoprotein receptor-related protein 8; *Vldlr*, very-low-density lipoprotein receptor; *Gad1*, glutamic acid decarboxylase 1 (glutamic acid decarboxylase 67); *Pax6*, paired box 6; *Eomes*, eomesodermin homolog (T-box brain protein 2); *Dpysl3*, dihydropyrimidinase-like 3.

[a]Mean ± SD ($n = 5$) relative to the expression levels in untreated controls. Real-time PCR analysis of *Hprt* and *Gapdh* was performed for the analysis of each target gene.

Significantly different from the untreated controls by Student's or Aspin-Welch's *t*-test ($p < 0.01$).

than that induced by maternal protein restriction, and therefore, it did not affect neurogenesis and interneuron distribution. On the other hand, we found offspring deaths during and after Mn exposure in all dosed groups without relation to the dose of Mn, irrespective of the lack of apparent general toxicity in dams and offspring except for the systemic growth retardation of offspring. The largest numbers of deaths were observed at the middle dose showing more hyperactive and aggressive behavior as compared with the highest dose. Although offspring deaths have not been reported due to excess Mn exposure in experimental animals, we previously found offspring deaths showing similar hyperactive and aggressive behavior as well as sustained aberration of neurogenesis after developmental hypothyroidism in rats (Saegusa *et al.*, 2010; Shibutani *et al.*, 2009). Therefore, developmental effect of Mn on the brain may be related to offspring deaths. Of note, mouse pups may gradually start to consume diet from around PND 10, and therefore, mg-test-substance per kg-BW basis of pups may actually be consuming a higher dose than adult case during their second week of the lactation period.

Mn exposure via maternal milk from PNDs 4 to 21 caused Mn accumulation in the cerebellum, midbrain, and striatum in rat offspring (Garcia *et al.*, 2006). In the present study, we examined cerebellar tissue to represent brain concentration of Mn. We observed increased Mn concentrations in the cerebellum in male offspring with $\geq$ 32 ppm Mn at PND 21 to sustain higher Mn concentrations at PND 77 when compared with time-matched untreated controls, despite no concentration changes in dams. Exposure *in utero* and during lactation to inhaled $MnSO_4$ has been reported to increase Mn concentrations in the striatum and cerebellum of offspring at doses that do not change Mn concentrations in dams (Dorman *et al.*, 2005). Studies on experimental exposure to $MnCl_2$ revealed that Mn concentrations in the brain in developing rats were higher than that in adult rats at the same dose (Dorman *et al.*, 2000; Takeda *et al.*, 1999). The increase in offspring brain Mn concentrations may be related to increased Mn absorption from the juvenile gastrointestinal tract as well as an incompletely formed neonatal blood-brain barrier and a virtual absence of excretory mechanisms until weaning (Dorman *et al.*, 2000). These results suggest that offspring are rather unprotected against developmental exposure to Mn, in contrast to adult animals that have protective functions against ingested Mn even at high doses. Therefore, only offspring are at risk of neurotoxicity, which includes impaired neuronal differentiation by maternal Mn exposure. Interestingly, an *in vitro* study using astrocyte-neuron cocultures has shown that $MnCl_2$ inhibited the ability of astrocytes to promote neurite outgrowth of hippocampal neuronal precursor cells (Giordano *et al.*, 2009). This result may be related to the decrease of immature granule cells in the SGZ at the end of exposure in the present study. Because immature granule cells already have dendritic growth cones and recurrent basal dendrites (Ribak *et al.*, 2004), immature granule cells may be the target of Mn, which suppresses differentiation into mature granule cells causing apoptosis.

In the present study, we detected a mild reduction in the serum concentration of T_4 in male offspring on weaning after developmental Mn exposure at 800 ppm, whereas there were no changes in the serum concentrations of T_3 and TSH. This T_4 reduction did not last into the adult stage. In contrast, a dietary study of rats treated with 10 mg/kg/day of $MnSO_4$ (3.6 mg/kg/day as Mn) for 5 weeks resulted in a significant decrease in serum T_3, T_4, and TSH concentrations, and a 2-year study of Mn in mice with a dose of 584 mg/kg/day $MnSO_4$ (213 mg/kg/day as Mn) increased the incidence of hyperplasia and dilatation of thyroid follicles (reviewed in Soldin and Aschner, 2007). These results suggest an antithyroid effect of Mn; however, our present study indicates a weak antithyroid effect. Interestingly, lactational Mn exposure study reporting Mn accumulation in the brain of rat offspring at a dietary dose of 100 ppm Mn showed a slightly reduced brain Fe-concentration (Garcia *et al.*, 2006). Because perinatal Fe deficiency has shown to cause reduced neonatal rat circulating and brain thyroid hormone concentrations as well as brain Fe concentration (Bastian *et al.*, 2010), thyroid hormone status may be affected by excess Mn exposure. However, we did not observe any changes in cerebellar Fe concentrations by Mn exposure even at 800 ppm in offspring in the present study, whereas the reason for the discrepancy between the above mentioned study and ours was not clear. On the other hand, we previously

observed similar hippocampal interneuron changes during developmental hypothyroidism, accompanied with striking antithyroid effects on serum thyroid–related hormones using rats (Saegusa *et al.*, 2010). However, the magnitude of brain changes was similar to the Mn-exposed cases observed here. Therefore, hypothyroidism may not be the major cause of developmental neuronal effects by Mn.

In the present study, the rodent chow contained high concentrations of Mn (4.84 mg/100 g MF basal diet). This dietary level provides a daily Mn intake of 8.6–17.3 mg/kg BW during gestation and lactation periods in dams of untreated controls. As mentioned earlier, the ESADDI of Mn has been estimated to be approximately 0.6 mg/day at 7–12 months of age, 1.2 mg/day at 1–3 years of age, 1.5 mg/day at 4–8 years of age, and 2–5 mg/day for adults. For newborns, the ESADDI has been estimated to be 0.003 mg/day, less than that for adults or children (Aschner and Aschner, 2005). Therefore, developmental exposure studies in rodents are performed with extremely high-basal Mn-intake levels as compared with human counterparts. In the present study, we found an increase of reelin-synthesizing interneurons in the dentate gyrus following treatment with 160 ppm Mn at PND 21. Of note, this Mn exposure level provides only a 2.1- to 2.5-fold increase in the daily intake of Mn when compared with untreated control animals, which is a small difference in exposure levels.

In conclusion, developmental Mn exposure in the form of $MnCl_2 \cdot xH_2O$ in mice induced an increase in apoptosis, which targeted immature granule cells during development. To this effect, the relationship to developmental hypothyroidism may be small. The sustained increase in immature reelin-synthesizing GABAergic interneurons may be a sign of continued aberration in neurogenesis and following neuronal migration, which causes the overproduction of immature granule cells at the adult stage. Increased NeuN-expressing neurons in the hilus at the adult stage may represent mature interneurons that stop producing reelin but facilitate differentiation of progenitor cells to immature granule cells. Sustained high concentrations of Mn in the brain may be responsible for these changes. Because neurogenesis in the hippocampal dentate gyrus continues during postnatal life, there is a possibility that excess Mn affects neurogenesis even at the adult stages.

SUPPLEMENTARY DATA

Supplementary data are available online at http://toxsci.oxfordjournals.org/.

FUNDING

Health and Labor Sciences Research Grants (Research on Risk of Chemical Substances) from the Ministry of Health, Labor, and Welfare of Japan.

ACKNOWLEDGMENTS

The authors thank Mrs Shigeko Suzuki for her technical assistance in preparing the histological specimens. The authors disclose that there are no competing financial interests that could inappropriately influence the outcome of this study.

REFERENCES

Aschner, J. L., and Aschner, M. (2005). Nutritional aspects of manganese homeostasis. *Mol. Aspects Med.* **26,** 353–362.

Bastian, T. W., Prohaska, J. R., Georgieff, M. K., and Anderson, G. W. (2010). Perinatal iron and copper deficiencies alter neonatal rat circulating and brain thyroid hormone concentrations. *Endocrinology* **151,** 4055–4065.

Breunig, J. J., Silbereis, J., Vaccarino, F. M., Sestan, N., and Rakic, P. (2007). Notch regulates cell fate and dendrite morphology of newborn neurons in the postnatal dentate gyrus. *Proc. Natl. Acad. Sci. U.S.A.* **104,** 20558–20563.

Chandra, S. V., and Shukla, G. S. (1978). Manganese encephalopathy in growing rats. *Environ. Res.* **15,** 28–37.

D'Arcangelo, G., Nakajima, K., Miyata, T., Ogawa, M., Mikoshiba, K., and Curran, T. (1997). Reelin is a secreted glycoprotein recognized by the CR-50 monoclonal antibody. *J. Neurosci.* **17,** 23–31.

Dobson, A. W., Erikson, K. M., and Aschner, M. (2004). Manganese neurotoxicity. *Ann. N. Y. Acad. Sci.* **1012,** 115–128.

Dorman, D. C., McElveen, A. M., Marshall, M. W., Parkinson, C. U., James, R. A., Struve, M. F., and Wong, B. A. (2005). Tissue manganese concentrations in lactating rats and their offspring following combined in utero and lactation exposure to inhaled manganese sulfate. *Toxicol. Sci.* **84,** 12–21.

Dorman, D. C., Struve, M. F., Vitarella, D., Byerly, F. L., Goetz, J., and Miller, R. (2000). Neurotoxicity of manganese chloride in neonatal and adult CD rats following subchronic (21-day) high-dose oral exposure. *J. Appl. Toxicol.* **20,** 179–187.

Garcia, S. J., Gellein, K., Syversen, T., and Aschner, M. (2006). A manganese-enhanced diet alters brain metals and transporters in the developing rat. *Toxicol. Sci.* **92,** 516–525.

Giordano, G., Pizzurro, D., VanDeMark, K., Guizzetti, M., and Costa, L. G. (2009). Manganese inhibits the ability of astrocytes to promote neuronal differentiation. *Toxicol. Appl. Pharmacol.* **240,** 226–235.

Gong, C., Wang, T. W., Huang, H. S., and Parent, J. M. (2007). Reelin regulates neuronal progenitor migration in intact and epileptic hippocampus. *J. Neurosci.* **27,** 1803–1811.

Goodman, J. H., and Gilbert, M. E. (2007). Modest thyroid hormone insufficiency during development induces a cellular malformation in the corpus callosum: A model of cortical dysplasia. *Endocrinology* **148,** 2593–2597.

Hack, I., Hellwig, S., Junghans, D., Brunne, B., Bock, H. H., Zhao, S., and Frotscher, M. (2007). Divergent roles of ApoER2 and Vldlr in the migration of cortical neurons. *Development* **134,** 3883–3891.

Hodge, R. D., Kowalczyk, T. D., Wolf, S. A., Encinas, J. M., Rippey, C., Enikolopov, G., Kempermann, G., and Hevner, R. F. (2008). Intermediate progenitors in adult hippocampal neurogenesis: Tbr2 expression and coordinate regulation of neuronal output. *J. Neurosci.* **28,** 3707–3717.

Khan, K., Factor-Litvak, P., Wasserman, G. A., Liu, X., Ahmed, E., Parvez, F., Slavkovich, V., Levy, D., Mey, J., van Geen, A., *et al.* (2011). Manganese exposure from drinking water and children's classroom behavior in Bangladesh. *Environ. Health Perspect.* **119,** 1501–1506.

Kitazawa, M., Anantharam, V., Yang, Y., Hirata, Y., Kanthasamy, A., and Kanthasamy, A. G. (2005). Activation of protein kinase C delta by

proteolytic cleavage contributes to manganese-induced apoptosis in dopaminergic cells: Protective role of Bcl-2. *Biochem. Pharmacol.* **69,** 133–146.

Knoth, R., Singec, I., Ditter, M., Pantazis, G., Capetian, P., Meyer, R. P., Horvat, V., Volk, B., and Kempermann, G. (2010). Murine features of neurogenesis in the human hippocampus across the lifespan from 0 to 100 years. *PLoS One* **5,** e8809.

Kontur, P. J., and Fechter, L. D. (1988). Brain regional manganese levels and monoamine metabolism in manganese-treated neonatal rats. *Neurotoxicol. Teratol.* **10,** 295–303.

Lavado-Autric, R., Ausó, E., García-Velasco, J. V., Arufe Mdel, C., del Rey, F. E., Berbel, P., and de Escobar, G. M. (2003). Early maternal hypothyroxinemia alters histogenesis and cerebral cortex cytoarchitecture of the progeny. *J. Clin. Invest.* **111,** 954–957.

Livak, K. J., and Schmittgen, T. D. (2001). Analysis of relative gene expression data using real-time quantitative PCR and the $2^{-\Delta\Delta CT}$ method. *Methods* **25,** 402–408.

Lussier, A. L., Caruncho, H. J., and Kalynchuk, L. E. (2009). Repeated exposure to corticosterone, but not restraint, decreases the number of reelin-positive cells in the adult rat hippocampus. *Neurosci. Lett.* **460,** 170–174.

Montaron, M. F., Koehl, M., Lemaire, V., Drapeau, E., Abrous, D. N., and Le Moal, M. (2004). Environmentally induced long-term structural changes: Cues for functional orientation and vulnerabilities. *Neurotox. Res.* **6,** 571–580.

Mullen, R. J., Buck, C. R., and Smith, A. M. (1992). NeuN a neuronal specific nuclear protein in vertebrates. *Development* **116,** 201–211.

Ogawa, B., Ohishi, T., Wang, L., Takahashi, M., Taniai, E., Hayashi, H., Mitsumori, K., and Shibutani, M. (2011). Disruptive neuronal development by acrylamide in the hippocampal dentate hilus after developmental exposure in rats. *Arch. Toxicol.* **85,** 987–994.

Ohishi, T., Wang, L., Ogawa, B., Fujisawa, K., Taniai, E., Hayashi, H., Mitsumori, K., and Shibutani, M. (2010). No effect of sustained systemic growth retardation on the distribution of reelin-expressing interneurons in the neuron-producing hippocampal dentate gyrus in rats. *Reprod. Toxicol.* **30,** 591–599.

Pawluski, J. L., Brummelte, S., Barha, C. K., Crozier, T. M., and Galea, L. A. (2009). Effects of steroid hormones on neurogenesis in the hippocampus of the adult female rodent during the estrous cycle, pregnancy, lactation and aging. *Front. Neuroendocrinol.* **30,** 343–357.

Ramos-Moreno, T., Galazo, M. J., Porrero, C., Martínez-Cerdeño, V., and Clascá, F. (2006). Extracellular matrix molecules and synaptic plasticity: Immunomapping of intracellular and secreted Reelin in the adult rat brain. *Eur. J. Neurosci.* **23,** 401–422.

Reznikov, K. Y. (1991). Cell proliferation and cytogenesis in the mouse hippocampus. *Adv. Anat. Embryol. Cell Biol.* **122,** 1–74.

Ribak, C. E., Korn, M. J., Shan, Z., and Obenaus, A. (2004). Dendritic growth cones and recurrent basal dendrites are typical features of newly generated dentate granule cells in the adult hippocampus. *Brain Res.* **1000,** 195–199.

Saegusa, Y., Woo, G.-H., Fujimoto, H., Kemmochi, S., Shimamoto, K., Hirose, M., Mitsumori, K., Nishikawa, A., and Shibutani, M. (2010). Sustained production of Reelin-expressing interneurons in the hippocampal dentate hilus after developmental exposure to anti-thyroid agents in rats. *Reprod. Toxicol.* **29,** 407–414.

Schoonover, C. M., Seibel, M. M., Jolson, D. M., Stack, M. J., Rahman, R. J., Jones, S. A., Mariash, C. N., and Anderson, G. W. (2004). Thyroid hormone regulates oligodendrocyte accumulation in developing rat brain white matter tracts. *Endocrinology* **145,** 5013–5020.

Seki, T. (2002). Expression patterns of immature neuronal markers PSA-NCAM, CRMP-4 and NeuroD in the hippocampus of young adult and aged rodents. *J. Neurosci. Res.* **70,** 327–334.

Shibutani, M., Lee, K.-Y., Igarashi, K., Woo, G.-H., Inoue, K., Nishimura, T., and Hirose, M. (2007). Hypothalamus region-specific global gene expression profiling in early stages of central endocrine disruption in rat neonates injected with estradiol benzoate or flutamide. *Dev. Neurobiol.* **67,** 253–269.

Shibutani, M., Uneyama, C., Miyazaki, K., Toyoda, K., and Hirose, M. (2000). Methacarn fixation: A novel tool for analysis of gene expressions in paraffin-embedded tissue specimens. *Lab. Invest.* **80,** 199–208.

Shibutani, M., Woo, G.-H., Fujimoto, H., Saegusa, Y., Takahashi, M., Inoue, K., Hirose, M., and Nishikawa, A. (2009). Assessment of developmental effects of hypothyroidism in rats from in utero and lactation exposure to anti-thyroid agents. *Reprod. Toxicol.* **28,** 297–307.

Soldin, O. P., and Aschner, M. (2007). Effects of manganese on thyroid hormone homeostasis: Potential links. *Neurotoxicology* **28,** 951–956.

Steel, R. G. D. (1959). A multiple comparison rank sum test: Treatments versus control. *Biometrics* **15,** 560–572.

Takeda, A., Ishiwatari, S., and Okada, S. (1999). Manganese uptake into rat brain during development and aging. *J. Neurosci. Res.* **56,** 93–98.

Tozuka, Y., Fukuda, S., Namba, T., Seki, T., and Hisatsune, T. (2005). GABAergic excitation promotes neuronal differentiation in adult hippocampal progenitor cells. *Neuron* **47,** 803–815.

Wierońska, J. M., Brański, P., Siwek, A., Dybala, M., Nowak, G., and Pilc, A. (2010). GABAergic dysfunction in mGlu7 receptor-deficient mice as reflected by decreased levels of glutamic acid decarboxylase 65 and 67kDa and increased reelin proteins in the hippocampus. *Brain Res.* **1334,** 12–24.

Arch Toxicol
DOI 10.1007/s00204-012-0846-y

REPRODUCTIVE TOXICOLOGY

Similar distribution changes of GABAergic interneuron subpopulations in contrast to the different impact on neurogenesis between developmental and adult-stage hypothyroidism in the hippocampal dentate gyrus in rats

Ayako Shiraki · Hirotoshi Akane · Takumi Ohishi · Liyun Wang · Reiko Morita · Kazuhiko Suzuki · Kunitoshi Mitsumori · Makoto Shibutani

Received: 29 February 2012 / Accepted: 14 March 2012

Abstract Hypothyroidism affects neurogenesis. The present study was performed to clarify the sensitivity of neurogenesis-related cellular responses in the hippocampal dentate gyrus between developmental and adult-stage hypothyroidism. An exposure study of methimazole (MMI) as an anti-thyroid agent at 0, 50, 200 ppm in the drinking water was performed using pregnant rats from gestation day 10 to postnatal day (PND) 21 (developmental hypothyroidism) and adult male rats by setting an identical exposure period from PND 46 through to PND 77 (adult-stage hypothyroidism). Offspring with developmental hypothyroidism were killed at PND 21 or PND 77, and animals with adult-stage hypothyroidism were killed at PND 77. Proliferation and apoptosis were unchanged in the dentate subgranular zone by either developmental or adult-stage hypothyroidism. With regard to precursor granule cells, a sustained reduction of paired box 6-positive stem or early progenitor cells and a transient reduction of doublecortin-positive late-stage progenitor cells were observed after developmental hypothyroidism with MMI at 50 and 200 ppm. These cells were unchanged by adult-stage hypothyroidism. With regard to γ-aminobutyric acid (GABA) ergic interneuron subpopulations in the dentate hilus, the number of parvalbumin-positive cells was decreased and the number of calretinin-positive cells was increased after both developmental and adult-stage hypothyroidism with MMI at 50 and 200 ppm. Fluctuations in GABAergic interneuron numbers with developmental hypothyroidism continued through to PND 77 with 200 ppm MMI. Considering the roles of GABAergic interneuron subpopulations in neurogenesis and neuronal differentiation, subpopulation changes in GABAergic interneurons by hypothyroidism may be the signature of aberrant neurogenesis even at the adult stage.

Keywords Hypothyroidism · Hippocampal dentate gyrus · Impaired neurogenesis · γ-Aminobutyric acid (GABA) ergic interneurons · Parvalbumin (Pvalb)

Abbreviations

ADHD	Attention deficit and hyperactivity disorder
Calb2	Calretinin
C_T	Threshold cycle
Dcx	Doublecortin
GABA	γ-Aminobutyric acid
GD	Gestational day
Hprt	Hypoxanthine-guanine phosphoribosyltransferase
MMI	Methimazole
Pax6	Paired box 6
PCNA	Proliferating cell nuclear antigen
PND	Postnatal day
Pvalb	Parvalbumin
PTU	6-propyl-2-thiouracil
SD	Sprague–Dawley
SGZ	Subgranular zone
T_3	Triiodothyronine
T_4	Thyroxine
TH	Thyroid hormone
TSH	Thyroid-stimulating hormone

Electronic supplementary material The online version of this article (doi:10.1007/s00204-012-0846-y) contains supplementary material, which is available to authorized users.

A. Shiraki · H. Akane · T. Ohishi · L. Wang · R. Morita · K. Suzuki · K. Mitsumori · M. Shibutani (✉)
Laboratory of Veterinary Pathology, Tokyo University of Agriculture and Technology, 3-5-8 Saiwai-cho, Fuchu-shi, Tokyo 183-8509, Japan
e-mail: mshibuta@cc.tuat.ac.jp

Published online: 31 March 2012

TUNEL Terminal deoxynucleotidyl transferase dUTP nick end labeling

Introduction

Thyroid hormones (THs) play a crucial role in normal brain development during fetal and neonatal periods. They have many effects relating to neural proliferation, cell migration, neuronal differentiation, and synaptogenesis (Bernal and Nunez 1995). In humans, fetal and postnatal TH deficiency may cause mental retardation and attention deficit and hyperactivity disorder (ADHD) (Delange 2000; Vermiglio et al. 2004). TH is also essential for brain function in adulthood. Adult-stage hypothyroidism is linked to anxiety and depression, as well as impaired learning and memory (Almeida et al. 2007; Sait Gönen et al. 2004).

Experimentally, developmental hypothyroidism induces neurological deficits, learning impairments, memory dysfunction (Pineda-Reynoso et al. 2010; Akaike et al. 1991), and ADHD-like behaviors (Negishi et al. 2005). Rat offspring exposed maternally to anti-thyroid agents such as 6-propyl-2-thiouracil (PTU) and methimazole (MMI) show aberrant brain growth, resulting in an impairment of neuronal migration as well as white matter hypoplasia involving limited axonal myelination and oligodendrocytic accumulation (Lavado-Autric et al. 2003; Schoonover et al. 2004; Goodman and Gilbert 2007). In addition, experimental induction of hypothyroidism in adult rats affects cell morphology and brain function, leading to depression-like behaviors (Koromilas et al. 2010, Montero-Pedrazuela et al. 2006). Thus, pharmacological induction of hypothyroidism in rats during the developmental stage and the adult stage may provide experimental models for ADHD and anxiety, respectively.

The hippocampus is involved in crucial neuronal networks responsible for cognitive, emotional and memory function. In the hippocampal formation, the subgranular zone (SGZ) of the dentate gyrus retains the capacity to produce new neurons throughout adult life. This process is called adult neurogenesis (Eriksson et al. 1998) and raises the possibility that developmental susceptibility of the dentate gyrus to neurotoxicants may affect neurogenesis in adulthood as well as during development. There are increasing numbers of chemicals that have recently been revealed to affect proliferation and differentiation of progenitor cells in the SGZ through exposure in mice or rats during postnatal life (Choi et al. 2011; Hwang et al. 2011; Nam et al. 2011; Yan et al. 2011; Yoo et al. 2011).

In neurogenesis in the SGZ of the hippocampal dentate gyrus, type-1 stem cells undergo self-renewal to produce intermediate generations, in order: type-2a, type-2b, and type-3 cells. Type-3 cells undergo final mitosis to differentiate into immature granule cells, then into mature granule cells (Hodge et al. 2008). There are a number of neuronal stage-defining markers to define these cell types. Among them, paired box 6 (Pax6) is a marker for type-1 and type-2a progenitor cells (Breunig et al. 2007; Hodge et al. 2008). In contrast, doublecortin (Dcx) is expressed from type-2b progenitor cells to immature granule cells with peak expression in immature granule cells (Breunig et al. 2007; Knoth et al. 2010). Therefore, chemical effect on neurogenesis could be roughly evaluated using these two markers.

It is well known that there is interplay between interneurons and neurogenesis. The major interneuron populations of the dentate gyrus use γ-aminobutyric acid (GABA) as their major neurotransmitter. Basket cells and chandelier cells are a subpopulation of these interneurons that synthesize a calcium-binding protein, parvalbumin (Pvalb), and synapse directly onto the soma or initial axonal segment of principal cells of the hippocampus (Houser 2007). In addition, Pvalb-expressing cells are the most active interneurons. They express high levels of cytochrome *c* in the mitochondria, which represents high activity for GABAergic transmission (Gulyás et al. 2006). There also are calretinin (Calb2)-expressing neurons distributed in the dentate gyrus as another major interneuron population (Gulyás et al. 1996). Our previous studies have revealed that developmental hypothyroidism by maternal exposure to MMI or PTU in rats causes a sustained increase in immature interneurons in the hilar region of the dentate gyrus, reflecting aberration in neurogenesis and following migration of granule cell lineage (Saegusa et al. 2010). This result may suggest that the dentate gyrus is a useful region for evaluation of developmental neurotoxicity affecting neurogenesis in combination with analysis of interneuron subpopulations.

Understanding of the cellular and molecular mechanisms governing adult neurogenesis may provide an alternative tool to establish in vivo system for screening developmental neurotoxicants affecting neurogenesis, such as in the 28-day repeated-oral dose-toxicity study scheme. For this purpose, it is reasonable to compare the sensitivity of neurogenesis-related cellular responses against developmental neurotoxicants between developmental and adult-stage exposures. The present study thereby aimed to elucidate the sensitivity of cellular responses involved in neurogenesis of the hippocampal dentate gyrus by exposure of rats to MMI, using Pax6 and Dcx as neuronal stage-defining markers and Pvalb and Calb2 as interneuron markers. A young adult exposure model was compared with a developmental exposure model by setting an identical exposure period.

Materials and methods

Chemicals and animals

Methimazole (2-mercapto-1-methylimidazole: MMI; CAS No. 60-56-0) was purchased from Sigma Chemical Co. (St. Louis, MO, USA). Pregnant Sprague–Dawley (SD) rats and adult male SD rats were obtained from Japan SLC, Inc. (Hamamatsu, Japan) at gestational day (GD) 1 (observation of vaginal plug was designated as GD 0) and postnatal day (PND) 35 (where PND 0 is the day of delivery), respectively. Animals were housed individually in polycarbonate cages with wood chip bedding, in an air-conditioned animal room maintained on a 12 h light–dark cycle at a temperature at 23 ± 2 °C with a relative humidity of 55 ± 15 %. Animals were allowed free access to food and water throughout the experimental period. A pelleted basal diet (MF-diet; Oriental Yeast Co., Ltd., Tokyo, Japan) and tap water were provided during the 10-day acclimatization period.

Experimental design

Two experiments were carried out. In Experiment 1, MMI was administered to dams (developmental exposure). Twenty-four dams were randomly divided into three groups of eight dams each and treated with 0, 50, or 200 ppm of MMI in the drinking water from GD 10 to PND 21. Based on our previous studies that have shown apparent aberrations in neuronal development in the hippocampal structure in offspring (Shibutani et al. 2009; Saegusa et al. 2010), the highest dose in combination with the duration of MMI-treatment was determined as shown above. Each dam was housed with her litter individually, and body weights and food and water intakes were measured regularly. All litters were culled to 8 pups on PND 2, retaining the maximal number of males per litter. On PND 21, all dams and 3–4 male pups per litter were killed by exsanguination from the abdominal aorta under deep anesthesia with ether. The remaining animals were maintained until PND 77. From PND 21, all offspring consumed the basal diet and tap water. All pups were killed on PND 77.

In Experiment 2, male SD rats were randomly divided into three groups of ten animals each and treated with 0, 50, or 200 ppm MMI in the drinking water from PND 46 to PND 77 (adult-stage exposure). All animals were killed on PND 77 in the same way as Experiment 1.

All animal experiments were conducted in accordance with the "Guidelines for Proper Conduct of Animal Experiments" (Science Council of Japan, June 1, 2006) and the protocol was approved by the Animal Care and Use Committee of the Tokyo University of Agriculture and Technology.

Thyroid-related hormone measurement

Before killing, blood samples were collected from the abdominal aorta under anesthesia from dams and male offspring in Experiment 1 and adult animals in Experiment 2. Plasma was prepared and stored at −30 °C. Concentrations of thyroid-stimulating hormone (TSH), triiodothyronine (T_3) and thyroxine (T_4) were measured by the chemiluminescent enzyme immunoassay method with the use of DPC Immulyze (Siemens Healthcare Diagnostics Inc., IL, USA).

Histopathology, immunohistochemistry and apoptosis assays

For immunohistochemical analysis, brains of 10 male pups/group (1 or 2 pups/litter) at PND 21 and PND 77 in Experiment 1 and 10 animals/group in Experiment 2 were fixed in Bouin's solution overnight at room temperature. Coronal slices were routinely processed from brains of PND 21 and PND 77 at −3.0 and −3.5 mm from the bregma, respectively, for paraffin embedding.

Histopathological analysis was performed on the brain sections (3 μm in thickness) stained with hematoxylin and eosin.

Immunohistochemistry was performed on the brain sections (3 μm in thickness) with antibodies against proliferating cell nuclear antigen (PCNA; mouse monoclonal, clone PC10, 1:200, Dako, Glostrup, Denmark), paired box 6 (Pax6; mouse monoclonal, clone AD2.38, 1:500, Abcam Inc., Cambridge, UK), doublecortin (Dcx; rabbit polyclonal, 1:1,000, Abcam Inc.), parvalbumin (Pvalb; mouse monoclonal, 1:1,000, Millipore, Billerica, MA, USA), and calretinin (Calb2; mouse monoclonal, 1:100, LifeSpan Biosciences, Inc., Seattle, WA, USA). Antigen retrieval was applied for Pvalb and Calb2 antibodies by microwaving sections at 90 °C for 10 min in 10 mM citrate buffer (pH 6.0). No antigen retrieval was performed for the other antibodies. Immunodetection was carried out using a VECTASTAIN® Elite ABC kit (Vector Laboratories Inc., Burlingame, CA, USA) with 3,3′-diaminobenzidine/H_2O_2 as the chromogen. Sections were then counterstained with hematoxylin for microscopic examination.

In order to detect apoptosis, terminal deoxynucleotidyl transferase dUTP nick end labeling (TUNEL) was carried out using the ApopTag® Peroxidase In situ Apoptosis Detection kit (Millipore).

Analysis of immunolocalization and apoptotic cells

PCNA-, Pax6-, Dcx-, or TUNEL-positive cells distributed in the SGZ of the dentate gyrus were counted bilaterally and the number was normalized with the length of the SGZ

(Fig. 1). In the dentate hilus, Pvalb- and Calb2-positive cells were counted bilaterally and the number was normalized with the hilus area. For quantitative measurement of each immunoreactive cell, digital photographs were taken with a 20× or 40× objective using a BX51 microscope (Olympus Optical Co., Ltd., Tokyo, Japan) attached to a DP70 Digital Camera System (Olympus Optical Co., Ltd.), and quantitative measurements were performed using the WinROOF image analysis software package (Version 5.7, Mitani Corp., Fukui, Japan).

Real-time RT-PCR analysis

For real-time RT-PCR analysis, brains of 5 male pups/group in Experiment 1 at PND 21 and PND 77, and 6 males/group in Experiment 2 were fixed in methacarn solution for 6 h then dehydrated in 99.5 % ethanol at 4 °C overnight as described previously (Lee et al. 2006). Brains were coronally cut at the positions of +1 and −5 mm from the bregma. Cerebral cortical tissues were removed with tweezers, and whole hippocampi were dissected bilaterally. Dissected tissue samples were preserved in 99.5 % ethanol at −80 °C until analysis. Gene transcript levels for *Pax6* and *Dcx* in Experiment 1, and *Pvalb* and *Calb2* in both Experiment 1 and Experiment 2 were analyzed in the hippocampal tissues. Total RNA samples were extracted with the RNeasy Mini Kit (QIAGEN, Hilden, Germany), and first strand cDNA was synthesized using SuperScript™ III Reverse Transcriptase (Invitrogen Corp., Carlsbad, CA, USA). Then, real-time PCR analysis was performed using the Power SYBR® Green PCR Master Mix (Applied Biosystems Inc., Foster City, CA, USA) and the StepOnePlus™ Real-Time PCR System (Applied Biosystems Inc.). The PCR primers shown in Table 1 were designed using Primer Express software (Version 3.0; Applied Biosystems Inc.). Threshold cycle (C_T) values were first normalized to the housekeeping gene hypoxanthine guanine phosphoribosyltransferase (*Hprt*), as an endogenous control in the same sample, then used to calculate the relative differences in gene expression to a control C_T value by the $2^{-\Delta\Delta C_T}$ method (Livak and Schmittgen 2001).

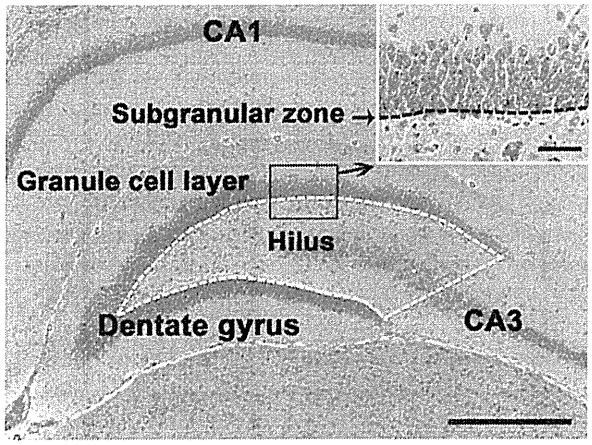

Fig. 1 Overview of the hippocampal formation of a male rat at PND 21 stained with hematoxylin and eosin. *Inset* shows the granule cell layer and SGZ at higher magnification. Number of Pvalb and Calb2 immunoreactive cells in the hilus (enclosed by the *white dotted line*) was counted and normalized for the unit area. Number of immunoreactive cells for PCNA, Pax6, Dcx, and the number of TUNEL-positive cells in the SGZ (shown by a *black dotted line*) was counted and normalized for the unit length. Objective magnification, ×4 (*inset* ×40). *Bar* 500 μm (*inset* 50 μm)

Statistical analysis

In Experiment 1, maternal data regarding the body and organ weights, food and water intake, and plasma concentrations of thyroid-related hormones were analyzed using the individual animal as the experimental unit. Offspring data regarding the body and organ weights were analyzed using the litter as the experimental unit. For data on thyroid-related hormone concentration, immunoreactive cell counts for each antigen or TUNEL-positive cells and real-time RT-PCR of pups, the individual animal was examined as the experimental unit. In Experiment 2, the individual animal was examined as the experimental unit for all data.

Differences in numerical data between the control and MMI-dosed groups in both Experiment 1 and 2 were evaluated in the following methods. First, the Bartlett's test

Table 1 Sequence of primers used for real-time RT-PCR

Gene	Accession no.	Forward primer (5′ → 3′)	Reverse primer (5′ → 3′)
Pax6	NM_013001	GCCCTCACCAACACGTACAGT	GGTTATTTGCCATGGTGAAGCT
Dcx	NM_053379	GGATTGTGTACGCTGTTTCTTCTG	TCAGGTCAGCCAGCAATGC
Pvalb	NM_022499	TCGCCACAAAAAGTTCTTCCA	TCTTCACATCATCCGCACTCTT
Calb2	NM_053988	AGCTCCAGGAGTACACCCAAAC	CCCAATTTGCCGTCTCCAT
Hprt	NM_012583	GCCGACCGGTTCTGTCAT	TCATAACCTGGTTCATCATCACTAATC

Pax6 paired box 6, *Dcx* doublecortin, *Pvalb* parvalbumin, *Calb2* calretinin, *Hprt* hypoxanthine guanine phosphoribosyltransferase

was used for the homogeneity of variance between the groups. If the variance was homologous, Dunnett's test was performed for comparison between groups. If there was a significant difference in variance, Steel's test was used instead.

The incidences of histopathological lesions in the brain were statistically compared using the Fisher's exact probability test.

Results

Maternal parameters (Experiment 1)

In the study of developmental exposure, there was one animal that was non-pregnant in both the untreated control and 50 ppm groups, and one dam that was moribund at GD 21 in both the 50 and 200 ppm groups. Moribund dams did not show brooding behavior after delivery, and all of their pups died. Therefore, non-pregnant rats and moribund dams were excluded from the experiment. Throughout the gestation period, there were no statistically significant differences in body weight or food and water intake between the untreated control dams and MMI-treated dams at both doses, except for a significant and slight decrease of food intake at GD 20 (Online Resource 1, Fig. s1a, b, c). After delivery of offspring, food and water intakes were significantly lower in the MMI-treated dams at both doses than in the untreated controls, except for the unchanged values in food intake at 200 ppm on PND 18 and in water intake at 200 ppm on PND 2 and at 50 ppm and 200 ppm on PND 7 (Online Resource 1, Fig. s1b, c). The MMI intakes of dams from GD 10 to GD 20 were 5.59 mg/kg body weight/day for 50 ppm and 22.38 mg/kg body weight/day for 200 ppm. From PND 1 to PND 21, the intake values were 7.19 mg/kg body weight/day for 50 ppm and 26.43 mg/kg body weight/day for 200 ppm.

Body weight, food intake and brain weight of offspring (Experiment 1)

Throughout the lactation period and after weaning to PND 77, body weights of the offspring in the MMI-exposed groups at both doses were significantly lower than the untreated control offspring (Online Resource 1, Fig. s2a). Food intake per animal was significantly lower in the 50 ppm MMI-exposed offspring after weaning (PND 21) to PND 35 and in the 200 ppm MMI-exposed offspring from PND 21 to PND 56 as compared with untreated control offspring (Online Resource 1, Fig. s2b). On PND 77, 200 ppm MMI-exposed offspring also showed significantly decreased food intake. On killing on PND 21, statistically significant decreases in the absolute brain weight and increases in relative brain weight were observed in MMI-exposed offspring at both doses (Online Resource 2, Table s1). A significant increase in relative brain weight was also observed in the 200 ppm MMI-exposed offspring at PND 77 (Online Resource 2, Table s1).

Body weight, food and water intake, MMI intake and brain weight of animals receiving adult-stage MMI exposure (Experiment 2)

The body weights of animals treated with MMI decreased significantly from PND 60 to PND 77 at both doses (Online Resource 1, Fig. s3a). Food intake after PND 46 and water intake after PND 53 also decreased significantly in MMI-treated groups at both doses (Online Resource 1, Fig. s3b, c). On killing on PND 77, there were no significant differences in the absolute brain weight in MMI-treated groups at both doses, while the relative brain weight at both doses showed significant increases compared to the untreated controls (Online Resource 2, Table s1). Amount of MMI intakes during exposure period were 4.26 mg/kg body weight/day for 50 ppm and 16.00 mg/kg body weight/day for 200 ppm.

Plasma levels of thyroid-related hormones

In the developmental exposure study (Experiment 1), statistically significant decreases of plasma T_3 and T_4 concentrations were evident in MMI-exposed offspring at both doses on PND 21 (Online Resource 2, Table s2). Plasma TSH concentration was significantly elevated in MMI-exposed offspring at both doses. At PND 77, no significant differences in thyroid-related hormones were observed between the untreated control offspring and MMI-exposed offspring at both doses.

In the adult-stage exposure study (Experiment 2), statistically significant decreases of plasma T_3 and T_4 concentrations and increase of TSH concentration were observed in MMI-exposed groups at both doses.

Table 2 Incidence of subcortical band heterotopia in the corpus callosum in Experiment 1

	MMI (ppm)		
	0 (cont)	50	200
No. of animals examined	10	10	10
PND 21	0	1	2
PND 77	0	2	9**

** Significantly different from the untreated controls by Fisher's exact probability test ($P < 0.01$)

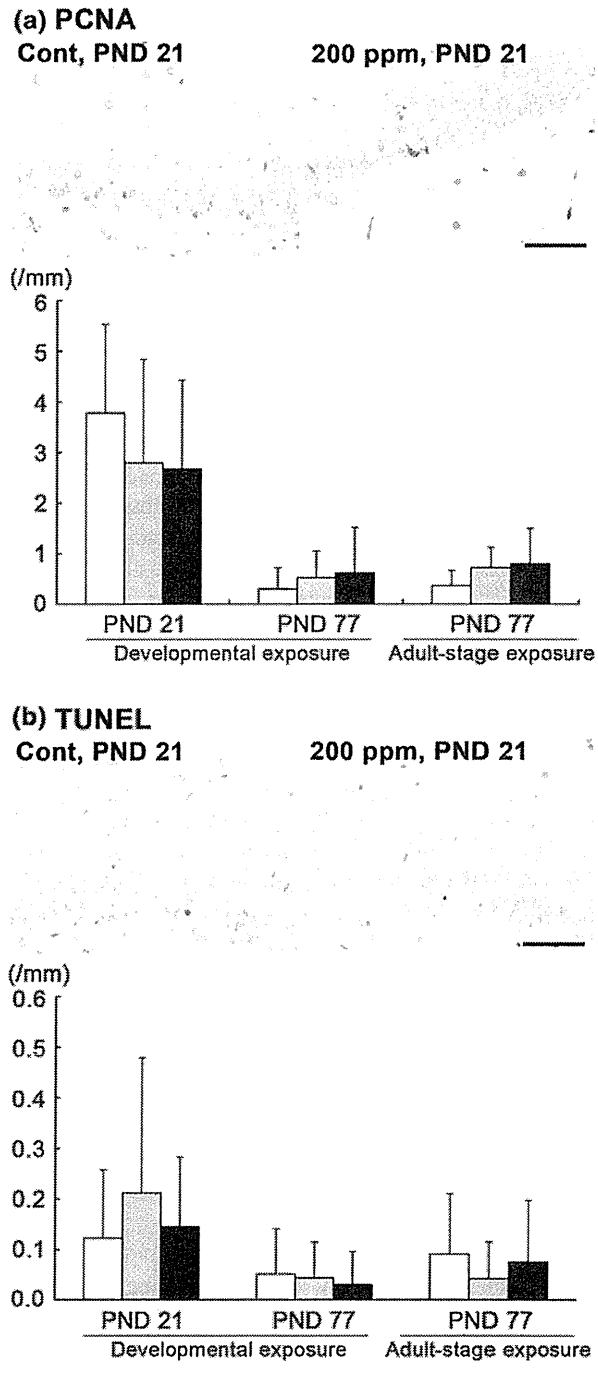

Fig. 2 Distribution and number of positive cells for PCNA-▶ immunohistochemistry and TUNEL-assay in the SGZ of offspring at PND 21 and PND 77 in Experiment 1 and animals at PND 77 in Experiment 2. **a** PCNA-positive cells in the SGZ at PND 21 of an offspring of the untreated controls (*left*) and an offspring exposed to 200 ppm MMI (*right*) in Experiment 1. Objective magnification, ×40. *Bar* 50 μm. The graph shows the number of PCNA-positive cells/unit length (mm) of the SGZ in bilateral hemispheres. **b** TUNEL-positive cells in the SGZ at PND 21 of offspring of untreated controls (*left*) and offspring exposed to 200 ppm MMI (*right*) in Experiment 1. Objective magnification, ×40. *Bar* 50 μm. The graph shows the number of TUNEL-positive cells/unit length (mm) of the SGZ in bilateral hemispheres. *White column* untreated controls, *gray column* 50 ppm MMI, *black column* 200 ppm MMI. $N = 10$

Histopathology of the brain

In the developmental exposure study (Experiment 1), subcortical band heterotopia was detected in the corpus callosum of MMI-exposed offspring at both doses on PND 21 and PND 77 (Table 2). Statistically significant increased incidence of this lesion was observed at 200 ppm on PND 77.

In the adult-stage exposure study (Experiment 2), development of subcortical band heterotopia was lacking by MMI-treatment.

Proliferating and apoptotic cell counts in the SGZ

In the developmental exposure study (Experiment 1), there were no significant differences in the number of either PCNA-positive proliferating cells or TUNEL-positive apoptotic cells in the SGZ between the untreated control offspring and MMI-exposed offspring at both doses on PND 21 and PND 77 (Fig. 2a, b).

In the adult-stage exposure study (Experiment 2), there were no significant differences in the number of both PCNA-positive cells and TUNEL-positive cells between the untreated controls and MMI-treated animals at both doses (Fig. 2a, b).

Neuronal progenitor cells in the SGZ

In the developmental exposure study (Experiment 1), statistically significant decreases in the number of Pax6-positive cells in the 200 ppm group and Dcx-positive cells in the 50 and 200 ppm groups were observed at PND 21 (Fig. 3a, b). At PND 77, the number of Pax6-positive cells was also significantly decreased in MMI-exposed offspring at both doses compared to the untreated control offspring, whereas there were no significant differences in the number of Dcx-positive cells in MMI-exposed offspring at both doses (Fig. 3a, b).

In the adult-stage exposure study (Experiment 2), no statistically significant changes in the number of Pax6- or Dcx-positive cells were observed between the untreated controls and MMI-treated animals at both doses (Fig. 3a, b).

GABAergic interneurons in the dentate hilus

In the developmental exposure study (Experiment 1), statistically significant decreases in the number of Pvalb-positive cells and increases in Calb2-positive cells were observed in MMI-exposed offspring at both doses on PND

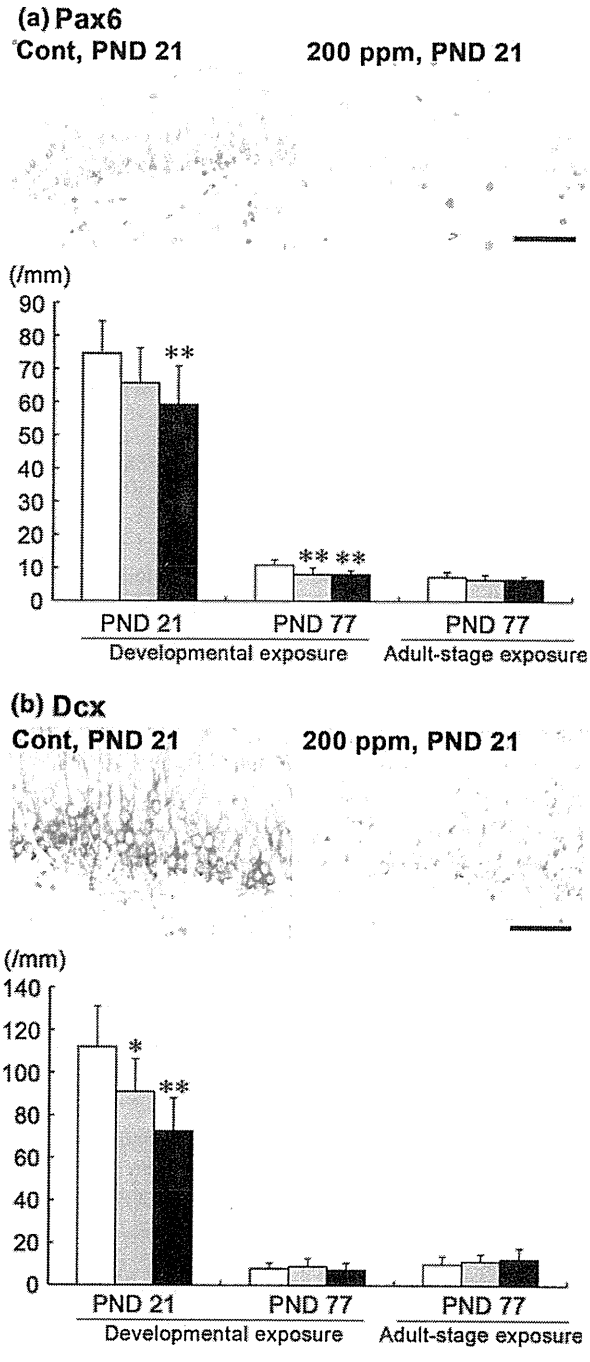

Fig. 3 Distribution and number of Pax6- and Dcx-immunoreactive ▶ cells in the SGZ of the dentate gyrus. **a** Pax6-positive cells in the SGZ at PND 21 of an offspring of the untreated controls (*left*) and an offspring exposed to 200 ppm MMI (*right*) in Experiment 1. Note the lower number of Pax6-positive cells in the offspring exposed to 200 ppm MMI compared with the control offspring. Objective magnification, ×40. *Bar* 50 μm. The graph shows the number of Pax6-positive cell/unit length (mm) of the bilateral hemispheres of offspring at PND 21 and PND 77 in Experiment 1 and animals at PND 77 in Experiment 2. **b** Dcx-positive cells in the SGZ at PND 21 of offspring of untreated controls (*left*) and offspring exposed to 200 ppm MMI (*right*) in Experiment 1. Note the lower number of Dcx-positive cells in the offspring exposed to 200 ppm MMI as compared with the control offspring. Objective magnification, ×40. *Bar* 50 μm. The graph shows the number of Dcx-positive cell/unit length (mm) of bilateral hemispheres of offspring at PND 21 and PND 77 in Experiment 1 and animals at PND 77 in Experiment 2. *White column* untreated controls, *gray column* 50 ppm MMI, *black column* 200 ppm MMI. $N = 10$. *, **Significantly different from the corresponding control animals by Dunnett's or Steel's test ($P < 0.05$; $P < 0.01$)

21 (Fig. 4a, b). At PND 77, a similar change was observed in the 200 ppm MMI-exposed offspring (Fig. 4a, b).

In the adult-stage exposure study (Experiment 2), the number of Pvalb-positive cells significantly decreased in MMI-treated animals at both doses, while the number of Calb2-positive cells showed a significant increase in MMI-treated animals at both doses (Fig. 4a, b).

Real-time RT-PCR data

In the developmental exposure study (Experiment 1), there were no statistically significant fluctuations in *Pax6* and *Dcx* mRNA levels between the untreated control offspring and MMI-exposed offspring at both doses on both PND 21 and PND 77 (Fig. 5a, b). However, the level of *Pvalb* mRNA significantly decreased at 200 ppm in MMI-exposed offspring on both PND 21 and PND 77 (Fig. 5a, b). There was a significant increase in transcript level of *Calb2* in 200 ppm MMI-exposed offspring at PND 21, whereas no significant difference was observed at PND 77 (Fig. 5a, b).

In the adult-stage exposure study (Experiment 2), mRNA levels of both *Pvalb* and *Calb2* showed no significant differences between the untreated controls and MMI-treated animals at both doses (Fig. 5c).

Discussion

In the present study, developmental hypothyroidism caused by maternal exposure to MMI induced subcortical band heterotopia in the corpus callosum as a result of aberrant neuronal migration due to TH insufficiency in offspring (Goodman and Gilbert 2007; Shibutani et al. 2009). In the SGZ, the number of Pax6-positive cells, one of the markers of early neuronal progenitors, decreased at both PND 21 and PND 77, while no apparent effect was observed in proliferation and apoptosis of progenitor cells at PND 21. A decrease in Dcx-positive cells was also observed at PND 21. In the dentate hilus, developmental hypothyroidism caused a decrease in Pvalb-positive cell number and an increase in Calb2-positive cells; at the high dose this increase was sustained into the adult stage. In contrast,

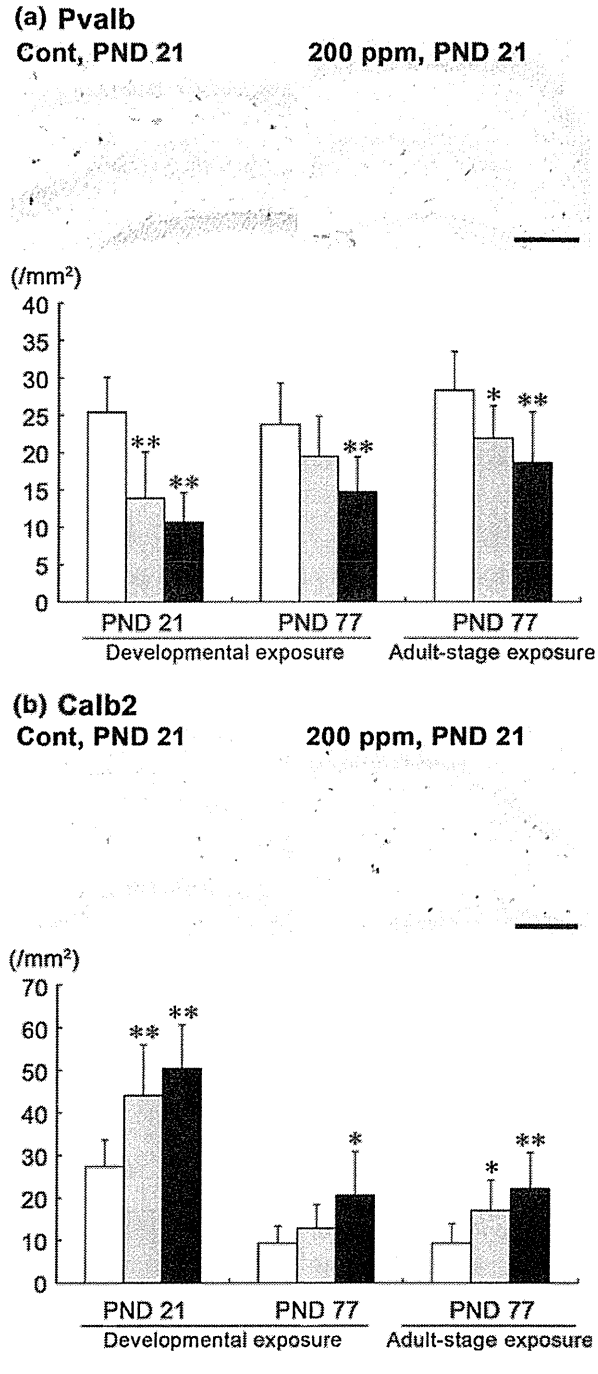

Fig. 4 Distribution and number of Pvalb- and Calb2-immunoreactive cells in the hilus of the dentate gyrus. **a** Pvalb-positive cells in the hilus of an offspring of untreated controls (*left*) at PND 21 and an offspring exposed to 200 ppm MMI (*right*) at PND 21 in Experiment 1. Note the lower number of Pvalb-positive cells in the offspring exposed to 200 ppm MMI as compared with the control offspring. Objective magnification, ×10. *Bar* 200 μm. The graph shows the number of Pvalb-positive cell/unit area (mm^2) of the bilateral hemispheres of offspring at PND 21 and PND 77 in Experiment 1 and animals at PND 77 in Experiment 2. **b** Calb2-positive cells in the hilus at PND 21 of offspring of untreated controls (*left*) and offspring exposed to 200 ppm MMI (*right*) in Experiment 1. Note the higher number of Calb2-positive cells in the offspring exposed to 200 ppm MMI as compared with the control offspring. Objective magnification, ×10. *Bar* 200 μm. The graph shows the number of Calb2-positive cell/unit area (mm^2) of the bilateral hemispheres of offspring at PND 21 and PND 77 in Experiment 1 and animals at PND 77 in Experiment 2. *White column* untreated controls, *gray column* 50 ppm MMI, *black column* 200 ppm MMI. $N = 10$. *, **Significantly different from the corresponding control animals by Dunnett's or Steel's test ($P < 0.05$; $P < 0.01$)

adult-stage hypothyroidism did not induce subcortical band heterotopia in the corpus callosum. There also were no changes in proliferation, apoptosis, or differentiation of progenitor cells in the SGZ, while interneuron populations in the hilus fluctuated similar to developmental hypothyroidism. To our knowledge, the present study was the first to show these interneuron population changes in adult-stage hypothyroidism (Wallis et al. 2008). Thus, even with adult-stage hypothyroidism, we found fluctuations in the number of interneurons similar to those observed in developmental hypothyroidism, while we did not detect any changes in neurogenesis.

It is well known that developmental hypothyroidism typically targets hippocampal neurogenesis in rats, causing impairment of granule cell maturation in the SGZ and irreversible reduction of the total number of granule cells in the dentate gyrus (Gong et al. 2010; Koromilas et al. 2010). In the present study, offspring at PND 21 after developmental hypothyroidism showed a sustained reduction of Pax6-positive cells, which represent type-1 stem cells and type-2a early stage progenitor cells in the SGZ, and a reduction of Dcx-positive cells, which represent the cell population from type-2b progenitor cells to immature granule cells in the SGZ. We also found thinning of the granule cell layer at both PND 21 and PND 77 in the present study (data not shown). These results may suggest that developmental hypothyroidism affects neuronal differentiation of newly generated earlier-stage progenitor cells in the SGZ, resulting in the reduction of mature granular cells. There may be a close relation between the affection of progenitor cell differentiation observed here and hypothyroidism-induced neuronal mismigration (Lavado-Autric et al. 2003; Shibutani et al. 2009). However, different from apparent effect on cell proliferation of progenitor cells by PTU-induced developmental hypothyroidism in our previous study (Saegusa et al. 2010), the effect of MMI-induced hypothyroidism on cell proliferation in the SGZ in the present study may be mild, because nascent cell proliferation activity as estimated by PCNA immunoreactivity was unchanged between euthyroid and hypothyroid cases at PND 21.

Because hypothyroidism targets stem cells and earlier progenitor cells as revealed in the present study, effect of

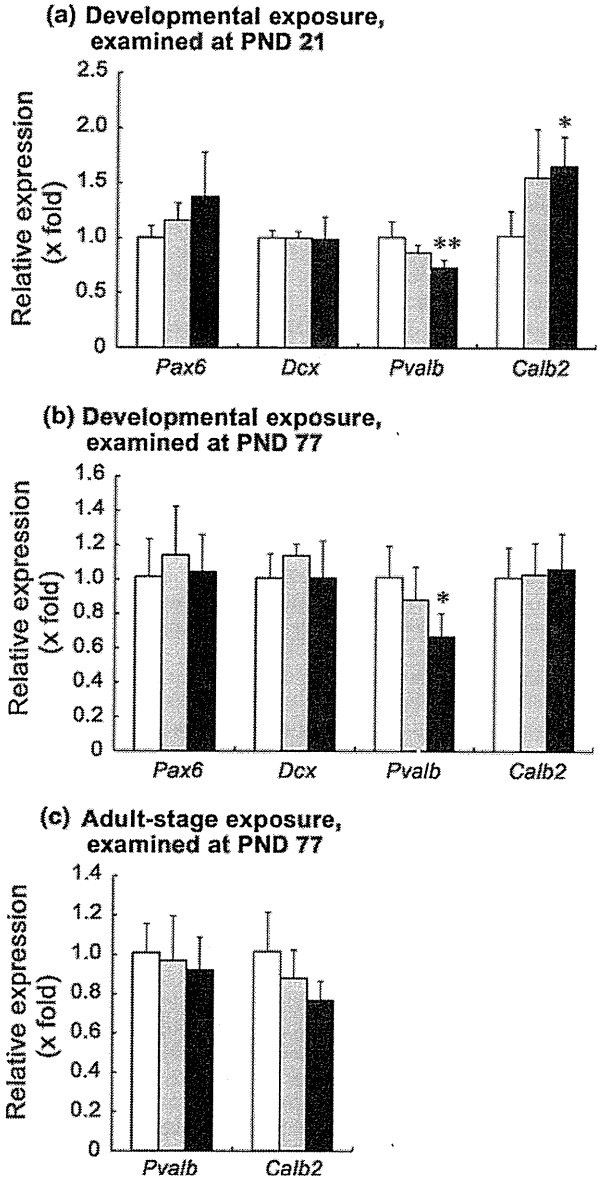

Fig. 5 The relative mRNA expression in the hippocampal tissue analyzed by real-time RT-PCR. **a** *Pax6*, *Dcx*, *Pvalb*, and *Calb2* in offspring at PND 21 in Experiment 1. **b** *Pax6*, *Dcx*, *Pvalb*, and *Calb2* of offspring at PND 77 in Experiment 1. **c** *Pvalb*, and *Calb2* in animals at PND 77 in Experiment 2. *White column* untreated controls, *gray column* 50 ppm MMI, *black column* 200 ppm MMI. $N = 5$ (Experiment 1), and 6 (Experiment 2). *, **Significantly different from the corresponding control animals by Dunnett's or Steel's test ($P < 0.05$; $P < 0.01$)

hypothyroidism on neurogenesis could be dependent on the activity of neurogenesis. Several studies have shown changes in adult neurogenesis in the hippocampal SGZ in rats with adult-stage hypothyroidism, such as decreases in newborn cell survival and differentiation (Ambrogini et al. 2005; Desouza et al. 2005; Zhang et al. 2009). However, these studies labeled progenitor cells by consecutive injections or continuous infusion of 5-bromo-2′-deoxyuridine, which may reflect a mild turnover of granule cells at the adult stage. Therefore, the impact of adult-stage hypothyroidism on adult neurogenesis in the present study may be so small that it cannot be detected by phenotype analysis using the neuronal stage-defining markers examined here.

A reduction in the number of Pvalb-positive cells and the GABAergic terminals was reported in TH receptor α1 (TRα1) mutant mice (Venero et al. 2005). Also, lack of T_3 during early development led to irreversible defects in the maturation of GABAergic systems, and Pvalb-positive interneurons especially showed delayed or incomplete maturation (Berbel et al. 1996; Gilbert et al. 2007; Wallis et al. 2008). Therefore, decreases in Pvalb-positive cells observed in both of the developmental and adult-stage hypothyroidism in the present study may be a reflection of reduced TH stimuli. In addition to inhibiting hippocampal granule cells, GABAergic interneurons play an important role in adult hippocampal neurogenesis (Duveau et al. 2011; Masiulis et al. 2011; Kapoor et al. 2011). Particularly, GABAergic interneurons provide direct neural inputs to type-2 progenitor cells in the SGZ and promote neural differentiation (Tozuka et al. 2005). Moreover, progenitor cell proliferation is promoted by the GABAergic system (Yoo et al. 2011). Therefore, in the present study, reduction of Pvalb-positive cells may lead to a decrease in GABAergic input onto SGZ progenitor cells, affecting neurogenesis even at the adult stage. However, we could detect changes in adult neurogenesis only after developmental hypothyroidism.

Pvalb-positive cells are known to have high average activity level and are considered to play a central role in inhibition of granule cells activity (Gulyás et al. 2006). A decrease in Pvalb-positive cells during development causes suppression of GABA-mediated granule cell inhibition (Gilbert et al. 2007). Moreover, TRα1 mutant mice showed anxiety, one of the symptoms recognized in both ADHD and anxiety syndrome in humans, as well as a decrease in the number of Pvalb-positive cells and GABAergic terminals (Venero et al. 2005). Therefore, the significantly decreased population of Pvalb-positive cells in both developmental and adult onset hypothyroidism in the present study may lead to symptoms of both ADHD and anxiety.

In the present study, an increase in the number of Calb2-positive cells was also observed in both developmental and adult-stage hypothyroidism. Of the several subtypes of GABAergic interneurons in the hippocampus, Calb2-positive interneurons are known to interconnect interneurons in the dentate gyrus and may coordinate the activity of the entire hippocampus by controlling the activity of inhibitory

neurons connecting to granule cells (Gulyás et al. 1996). Hence, the increase in Calb2-positive cells is considered to be secondary to the decrease in number of Pvalb-positive cells.

In conclusion, we found fluctuations in GABAergic interneuron subpopulations in both developmental and adult-stage hypothyroidism. While developmental hypothyroidism resulted in continued impairment of neurogenesis, we could not detect any apparent changes in neurogenesis in adult-stage hypothyroidism. Considering their role in neurogenesis, changes in GABAergic interneuron subpopulations may provide a sensitive tool for detection of aberrant neurogenesis. Our study also suggests that analysis of interneuron subpopulations may provide a tool for detection of changes in neurogenesis, particularly for regular toxicity tests such as the 28-day repeated-oral dose-toxicity test.

Acknowledgments The authors thank Mrs. Shigeko Suzuki for her technical assistance in preparing the histological specimens. This work was supported by a grant from Ministry of Economy, Trade and Industry (METI), Japan.

Conflict of interest All authors disclose that there are no conflicts of interest that could inappropriately influence the outcome of the present study.

References

Akaike M, Kato N, Ohno H, Kobayashi T (1991) Hyperactivity and spatial maze learning impairment of adult rats with temporary neonatal hypothyroidism. Neurotoxicol Teratol 13:317–322

Almeida C, Brasil MA, Costa AJ, Reis FA, Reuters V, Teixeira P, Ferreira M, Marques AM, Melo BA, Teixeira LB, Buescu A, Vaisman M (2007) Subclinical hypothyroidism: psychiatric disorders and symptoms. Rev Bras Psiquiatr 29:157–159

Ambrogini P, Cuppini R, Ferri P, Mancini C, Ciaroni S, Voci A, Gerdoni E, Gallo G (2005) Thyroid hormones affect neurogenesis in the dentate gyrus of adult rat. Neuroendocrinology 81:244–253

Berbel P, Marco P, Cerezo JR, DeFelipe J (1996) Distribution of parvalbumin immunoreactivity in the neocortex of hypothyroid adult rats. Neurosci Lett 204:65–68

Bernal J, Nunez J (1995) Thyroid hormones and brain development. Eur J Endocrinol 133:390–398

Breunig JJ, Silbereis J, Vaccarino FM, Sestan N, Rakic P (2007) Notch regulates cell fate and dendrite morphology of newborn neurons in the postnatal dentate gyrus. Proc Natl Acad Sci USA 104:20558–20563

Choi JH, Yoo KY, Lee CH, Yi SS, Yoo DY, Seong JK, Yoon YS, Hwang IK, Won MH (2011) Effects of treadmill exercise combined with MK 801 treatment on neuroblast differentiation in the dentate gyrus in rats. Cell Mol Neurobiol 31:285–292

Delange F (2000) The role of iodine in brain development. Proc Nutr Soc 59:75–79

Desouza LA, Ladiwala U, Daniel SM, Agashe S, Vaidya RA, Vaidya VA (2005) Thyroid hormone regulates hippocampal neurogenesis in the adult rat brain. Mol Cell Neurosci 29:414–426

Duveau V, Laustela S, Barth L, Gianolini F, Vogt KE, Keist R, Chandra D, Homanics GE, Rudolph U, Fritschy JM (2011) Spatiotemporal specificity of GABAA receptor-mediated regulation of adult hippocampal neurogenesis. Eur J Neurosci 34:362–373

Eriksson PS, Perfilieva E, Björk-Eriksson T, Alborn AM, Nordborg C, Peterson DA, Gage FH (1998) Neurogenesis in the adult human hippocampus. Nat Med 4:1313–1317

Gilbert ME, Sui L, Walker MJ, Anderson W, Thomas S, Smoller SN, Schon JP, Phani S, Goodman JH (2007) Thyroid hormone insufficiency during brain development reduces parvalbumin immunoreactivity and inhibitory function in the hippocampus. Endocrinology 148:92–102

Gong J, Liu W, Dong J, Wang Y, Xu H, Wei W, Zhong J, Xi Q, Chen J (2010) Developmental iodine deficiency and hypothyroidism impair neural development in rat hippocampus: involvement of doublecortin and NCAM-180. BMC Neurosci 11:50

Goodman JH, Gilbert ME (2007) Modest thyroid hormone insufficiency during development induces a cellular malformation in the corpus callosum: a model of cortical dysplasia. Endocrinology 148:2593–2597

Gulyás AI, Hájos N, Freund TF (1996) Interneurons containing calretinin are specialized to control other interneurons in the rat hippocampus. J Neurosci 16:3397–3411

Gulyás AI, Buzsáki G, Freund TF, Hirase H (2006) Populations of hippocampal inhibitory neurons express different levels of cytochrome c. Eur J Neurosci 23:2581–2594

Hodge RD, Kowalczyk TD, Wolf SA, Encinas JM, Rippey C, Enikolopov G, Kempermann G, Hevner RF (2008) Intermediate progenitors in adult hippocampal neurogenesis: Tbr2 expression and coordinate regulation of neuronal output. J Neurosci 28:3707–3717

Houser CR (2007) Interneurons of the dentate gyrus: an overview of cell types, terminal fields and neurochemical identity. Prog Brain Res 163:217–232

Hwang IK, Yoo KY, Yoo DY, Choi JH, Lee CH, Kang IJ, Kwon DY, Kim YS, Kim DW, Won MH (2011) Zizyphus enhances cell proliferation and neuroblast differentiation in the subgranular zone of the dentate gyrus in middle-aged mice. J Med Food 14:195–200

Kapoor R, Ghosh H, Nordstrom K, Vennstrom B, Vaidya VA (2011) Loss of thyroid hormone receptor β is associated with increased progenitor proliferation and NeuroD positive cell number in the adult hippocampus. Neurosci Lett 487:199–203

Knoth R, Singec I, Ditter M, Pantazis G, Capetian P, Meyer RP, Horvat V, Volk B, Kempermann G (2010) Murine features of neurogenesis in the human hippocampus across the lifespan from 0 to 100 years. PLoS ONE 5:e8809

Koromilas C, Liapi C, Schulpis KH, Kalafatakis K, Zarros A, Tsakiris S (2010) Structural and functional alterations in the hippocampus due to hypothyroidism. Metab Brain Dis 25:339–354

Lee KY, Shibutani M, Inoue K, Kuroiwa K, U M, Woo GH, Hirose M (2006) Methacarn fixation—effects of tissue processing and storage conditions on detection of mRNAs and proteins in paraffin-embedded tissues. Anal Biochem 351:36–43

Lavado-Autric R, Ausó E, García-Velasco JV, Arufe Mdel C, Escobar del Rey F, Berbel P, Morreale de Escobar G (2003) Early maternal hypothyroxinemia alters histogenesis and cerebral cortex cytoarchitecture of the progeny. J Clin Invest 111:1073–1082

Livak KJ, Schmittgen TD (2001) Analysis of relative gene expression data using real-time quantitative PCR and the $2^{-\Delta\Delta C_T}$ method. Methods 25:402–408

Masiulis I, Yun S, Eisch AJ (2011) The interesting interplay between interneurons and adult hippocampal neurogenesis. Mol Neurobiol. doi:10.1007/s12035-011-8207-z

Montero-Pedrazuela A, Venero C, Lavado-Autric R, Fernández-Lamo I, García-Verdugo JM, Bernal J, Guadaño-Ferraz A (2006) Modulation of adult hippocampal neurogenesis by thyroid hormones: implications in depressive-like behavior. Mol Psychiatry 11:361–371

Nam SM, Yoo DY, Kim W, Yoo M, Kim DW, Won MH, Hwang IK, Yoon YS (2011) Effects of s-allyl-L-cysteine on cell proliferation and neuroblast differentiation in the mouse dentate gyrus. J Vet Med Sci 73:1071–1075

Negishi T, Kawasaki K, Sekiguchi S, Ishii Y, Kyuwa S, Kuroda Y, Yoshikawa Y (2005) Attention-deficit and hyperactive neurobehavioural characteristics induced by perinatal hypothyroidism in rats. Behav Brain Res 159:323–331

Pineda-Reynoso M, Cano-Europa E, Blas-Valdivia V, Hernandez-Garcia A, Franco-Colin M, Ortiz-Butron R (2010) Hypothyroidism during neonatal and perinatal period induced by thyroidectomy of the mother causes depressive-like behavior in prepubertal rats. Neuropsychiatr Dis Treat 6:137–143

Saegusa Y, Woo GH, Fujimoto H, Kemmochi S, Shimamoto K, Hirose M, Mitsumori K, Nishikawa A, Shibutani M (2010) Sustained production of Reelin-expressing interneurons in the hippocampal dentate hilus after developmental exposure to antithyroid agents in rats. Reprod Toxicol 29:407–414

Sait Gönen M, Kisakol G, Savas Cilli A, Dikbas O, Gungor K, Inal A, Kaya A (2004) Assessment of anxiety in subclinical thyroid disorders. Endocr J 51:311–315

Schoonover CM, Seibel MM, Jolson DM, Stack MJ, Rahman RJ, Jones SA, Mariash CN, Anderson GW (2004) Thyroid hormone regulates oligodendrocyte accumulation in developing rat brain white matter tracts. Endocrinology 145:5013–5020

Shibutani M, Woo GH, Fujimoto H, Saegusa Y, Takahashi M, Inoue K, Hirose M, Nishikawa A (2009) Assessment of developmental effects of hypothyroidism in rats from in utero and lactation exposure to anti-thyroid agents. Reprod Toxicol 28:297–307

Tozuka Y, Fukuda S, Namba T, Seki T, Hisatsune T (2005) GABAergic excitation promotes neuronal differentiation in adult hippocampal progenitor cells. Neuron 47:803–815

Venero C, Guadaño-Ferraz A, Herrero AI, Nordström K, Manzano J, de Escobar GM, Bernal J, Vennström B (2005) Anxiety, memory impairment, and locomotor dysfunction caused by a mutant thyroid hormone receptor $\alpha 1$ can be ameliorated by T_3 treatment. Genes Dev 19:2152–2163

Vermiglio F, Lo Presti VP, Moleti M, Sidoti M, Tortorella G, Scaffidi G, Castagna MG, Mattina F, Violi MA, Crisà A, Artemisia A, Trimarchi F (2004) Attention deficit and hyperactivity disorders in the offspring of mothers exposed to mild-moderate iodine deficiency: a possible novel iodine deficiency disorder in developed countries. J Clin Endocrinol Metab 89:6054–6060

Wallis K, Sjögren M, van Hogerlinden M, Silberberg G, Fisahn A, Nordström K, Larsson L, Westerblad H, Morreale de Escobar G, Shupliakov O, Vennström B (2008) Locomotor deficiencies and aberrant development of subtype-specific GABAergic interneurons caused by an unliganded thyroid hormone receptor $\alpha 1$. J Neurosci 28:1904–1915

Yan BC, Yoo KY, Park JH, Lee CH, Choi JH, Won MH (2011) The high dosage of earthworm (*Eisenia andrei*) extract decreases cell proliferation and neuroblast differentiation in the mouse hippocampal dentate gyrus. Anat Cell Biol 44:218–225

Yoo DY, Kim W, Kim DW, Yoo KY, Chung JY, Youn HY, Yoon YS, Choi SY, Won MH, Hwang IK (2011) Pyridoxine enhances cell proliferation and neuroblast differentiation by upregulating the GABAergic system in the mouse dentate gyrus. Neurochem Res 36:713–721

Zhang L, Blomgren K, Kuhn HG, Cooper-Kuhn CM (2009) Effects of postnatal thyroid hormone deficiency on neurogenesis in the juvenile and adult rat. Neurobiol Dis 34:366–374

Reproductive Toxicology xxx (2012) xxx–xxx

Contents lists available at SciVerse ScienceDirect

Reproductive Toxicology

journal homepage: www.elsevier.com/locate/reprotox

Increased cellular distribution of vimentin and Ret in the cingulum induced by developmental hypothyroidism in rat offspring maternally exposed to anti-thyroid agents

Hitoshi Fujimoto[a], Gye-Hyeong Woo[a], Kaoru Inoue[a], Katsuhide Igarashi[b], Jun Kanno[b], Masao Hirose[c], Akiyoshi Nishikawa[d], Makoto Shibutani[a,e,*]

[a] Division of Pathology, National Institute of Health Sciences, 1–18–1 Kamiyoga, Setagaya-ku, Tokyo 158-8501, Japan
[b] Division of Molecular Toxicology, National Institute of Health Sciences, 1–18–1 Kamiyoga, Setagaya-ku, Tokyo 158-8501, Japan
[d] Biological Safety Research Center, National Institute of Health Sciences, 1–18–1 Kamiyoga, Setagaya-ku, Tokyo 158-8501, Japan
[c] Food Safety Commission, 5–2–20 Akasaka Park Bld. 22nd Floor, Akasaka, Minato-ku, Tokyo 107-6122, Japan
[e] Laboratory of Veterinary Pathology, Tokyo University of Agriculture and Technology, 3–5–8 Saiwai-cho, Fuchu-shi, Tokyo 183-8509, Japan

ARTICLE INFO

Article history:
Received 4 December 2011
Received in revised form 19 February 2012
Accepted 16 March 2012
Available online xxx

Keywords:
Developmental hypothyroidism
Cerebral white matter
Vimentin
Ret
Rat

ABSTRACT

To elucidate target molecules of white matter development responding to hypothyroidism, global gene expression profiling of cerebral white matter from male rat offspring was performed after maternal exposure to anti-thyroid agents, 6-propyl-2-thiouracil and methimazole, on postnatal day 20. Genes involved in central nervous system development commonly up- or down-regulated among groups treated with anti-thyroid agents. Immunohistochemical distributions of vimentin, Ret proto-oncogene (Ret), deleted in colorectal cancer protein (DCC), and Claudin11 (Cld11) were examined based on the gene expression profile. Immunoreactive cells for vimentin and Ret in the cingulum, and the immunoreactive intensity of Cld11 and DCC in whole white matter were increased by treatment with anti-thyroid agents. Immunoreactive cells for vimentin and Ret were immature astrocytes and oligodendrocytes, respectively. Thus, immunoreactive cells for vimentin and Ret may be quantitatively measurable targets of developmental hypothyroidism in white matter.

1. Introduction

Thyroid hormones are essential for normal fetal and neonatal brain development, control neuronal and glial proliferation in definitive brain regions and regulate neuronal migration and differentiation [1–3]. In humans, maternal hypothyroxinemia early in pregnancy may adversely affect fetal brain development, and importantly, even mild to moderate hypothyroxinemia may result in suboptimal neurodevelopment [4], thereby increasing the concern of impaired brain development induced by exposure to thyroid hormone-disrupting chemicals in the environment.

Developmental hypothyroidism leads to growth retardation, neurological defects and impaired performance in various behavioral learning actions [5,6]. Rat offspring maternally exposed to anti-thyroid agents, such as 6-propyl-2-thiouracil (PTU) and methimazole (MMI), show impaired brain growth including white matter hypoplasia with decreased axonal myelination and oligodendrocytes, and impairment of neurogenesis, neuronal migration, dendritic arborization and synapse formation [2,7–9]. These types of impaired brain growth are permanent and accompanied by apparent structural and functional abnormalities. However, the molecular mechanism of impaired brain growth is still unclear.

Histological lesion-specific gene expression profiling provides valuable information on the mechanisms underlying lesion development. In previous studies, we established molecular analysis methods for DNA, RNA and proteins in paraffin-embedded small tissue specimens using the organic solvent-based fixative methacarn, with high performance similar to that of unfixed frozen tissue specimens [10–12]. These methods have been used to analyze global gene expression changes in microdissected lesions [13–15].

Abbreviations: CC, corpus callosum; Cld11, claudin 11; CNS, central nervous system; DCC, deleted in colorectal cancer protein; GAPDH, glyceraldehyde 3-phosphate dehydrogenase; GD, gestation day; GDNF, glial cell line-derived neurotrophic factor; GFAP, glial fibrillary acidic protein; MMI, methimazole; OSP, oligodendrocyte specific protein; PCR, polymerase chain reaction; PND, postnatal day; PTU, 6-propyl-2-thiouracil; Ret, Ret proto-oncogene; RT, reverse transcription; v-Maf, v-maf musculoaponeurotic fibrosarcoma oncogene; Zfhx1b, zinc finger homeobox 1b.

* Corresponding author at: Laboratory of Veterinary Pathology, Tokyo University of Agriculture and Technology, 3–5–8 Saiwai-cho, Fuchu-shi, Tokyo 183-8509, Japan. Tel.: +81 42 367 5874; fax: +81 42 367 5771.
E-mail address: mshibuta@cc.tuat.ac.jp (M. Shibutani).

0890-6238/$ – see front matter © 2012 Elsevier Inc. All rights reserved.
http://dx.doi.org/10.1016/j.reprotox.2012.03.005

Please cite this article in press as: Fujimoto H, et al. Increased cellular distribution of vimentin and Ret in the cingulum induced by developmental hypothyroidism in rat offspring maternally exposed to anti-thyroid agents. Reprod Toxicol (2012), http://dx.doi.org/10.1016/j.reprotox.2012.03.005

To evaluate in vivo developmental brain growth effects of thyroid hormone-disrupting chemicals, we morphometrically analyzed neuronal migration and white matter development in a rat developmental hypothyroidism model [16]. Molecules involved in aberrant neurogenesis and neuronal mismigration were identified by global gene expression analysis of the hippocampal area [15]. In the present study, to elucidate marker molecules in white matter involved in developmental hypothyroidism, we performed global gene expression profiling using microarrays. To obtain the white matter-specific gene expression profile, a microdissection technique was applied to the corpus callosum (CC) and bilateral cerebral white matter. Based on expression profiles, cellular localization of selected molecules was then immunohistochemically examined in cerebral white matter after developmental exposure to anti-thyroid agents.

2. Materials and methods

2.1. Chemicals and animals

6-propyl-2-thiouracil (PTU; CAS No. 51-52-9) and methimazole (MMI; CAS No. 60-56-0) were purchased from Sigma Chemical Co. (St. Louis, MO). Pregnant CD® (SD) IGS rats at gestational day (GD) 3 (GD 0: the day vaginal plugs appeared) were purchased from Charles River Japan Inc. (Yokohama, Japan). Animals were individually housed in polycarbonate cages (SK-Clean, 41.5 cm × 26 cm × 17.5 cm; CLEA Japan Inc., Tokyo, Japan) with wood chip bedding (Sankyo Lab Service Corp., Tokyo, Japan) and maintained in a climate-controlled animal room (24 ± 1 °C, relative humidity: 55 ± 5%) with a 12 h light/dark cycle. A soy-free diet (Oriental Yeast Co. Ltd., Tokyo, Japan) was chosen as the basal diet for maternal animals to eliminate possible phytoestrogen effects [17]. Animals received food and water ad libitum throughout experimentation including a 1 week acclimation period.

2.2. Experimental design

Animal experiments are described elsewhere [16]. Briefly, maternal animals were randomly divided into four groups including an untreated control. Eight dams per group were treated with 3 or 12 ppm PTU or 200 ppm MMI, which was added to drinking water from GD 10 to postnatal day (PND) 20 (PND 0: the day of delivery). On PND 2, four male and four female offspring per dam were randomly selected and remaining litters were culled. On PND 20, 20 male and 20 female offspring (at least one male and one female per dam) per group were subjected to prepubertal necropsy [16,18]. All animals were weighed and sacrificed by exsanguination from the abdominal aorta under deep anesthesia with ether. Animal protocols were reviewed and approved by the Animal Care and Use Committee of the National Institute of Health Sciences, Japan.

2.3. Preparation of tissue specimens and microdissection

For microarray and real-time reverse transcription (RT)-polymerase chain reaction (PCR) analyses, the whole brain of male offspring was immediately removed at prepubertal necropsy on PND 20 ($n = 4$/group) and fixed with methacarn solution for 2 h at 4 °C [10]. Coronal brain slices taken at −3.5 mm from the bregma were dehydrated and embedded in paraffin. Embedded tissues were stored at 4 °C until tissue sectioning for microdissection [19].

For microdissection, 4 and 20 μm-thick serial sections were prepared. The 4 μm-thick sections were stained with hematoxylin and eosin for confirmation of anatomical orientation of the hippocampal substructure to aid microdissection (Fig. 1). The 20 μm-thick sections were mounted onto PEN-foil film (Leica Microsystems GmbH, Welzlar, Germany) overlaid on glass slides, dried in an incubator overnight at 37 °C, and then stained using an LCM staining kit (Ambion, Inc., Austin, TX). Regions of CC and bilateral cerebral white matter (external capsule) in sections, as shown in Fig. 1, were subjected to laser microbeam microdissection (Leica Microsystems GmbH). Forty sections from each animal were used for microdissection, and microdissected samples were individually stored in 1.5 ml tubes at −80 °C until total RNA extraction.

2.4. RNA preparation, amplification and microarray analysis

Total RNA extraction from microdissected regions, quantitation of RNA yield, and RNA amplification were performed using methods described elsewhere [14,15,19].

For microarray analysis, second-round-amplified biotin-labeled antisense RNAs were subjected to hybridization with a GeneChip® Rat Genome 230 2.0 Array (Affymetrix, Inc., Santa Clara, CA).

Gene selection and normalization of expression data were performed using GeneSpring® software 7.2 (Silicon Genetics, Redwood City, CA). Per chip normalization was performed according to a method described elsewhere [14,15]. Genes with expression changes of at least 2-fold in magnitude compared with those of untreated controls were selected. Common genes with altered expression in anti-thyroid agent exposed groups were also selected.

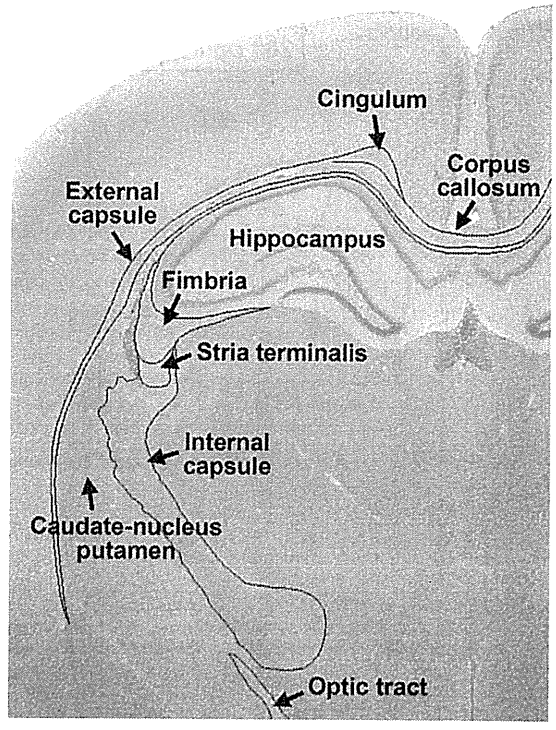

Fig. 1. Overview of the cerebral hemisphere of a male rat at PND 20 stained with hematoxylin and eosin. Magnification, 12.5×.

2.5. Real-time RT-PCR

Quantitative real-time RT-PCR using an ABI Prism 7900HT (Applied Biosystems Japan Ltd., Tokyo, Japan) was performed for confirmation of expression values obtained from microarray analysis. Selected genes showed altered expression (≥2-fold, ≤0.5-fold) in any of the anti-thyroid agent-exposed animals as compared with those of untreated controls. For example, vimentin, *Ret*, v-maf musculoaponeurotic fibrosarcoma oncogene (*v-Maf*) and tektin 4 as up-regulated genes, and *Cld11* and zinc finger homeobox 1b (*Zfhx1b*) as down-regulated ones. RT was performed using first-round antisense RNAs prepared for microarray analysis. For real-time PCR analysis, ABI Assays-on-Demand™ TaqMan® probe and primer sets from Applied Biosystems ($n = 4$/group) were used. For quantification of expression data, a standard curve method was applied. Expression values were normalized to glyceraldehyde 3-phosphate dehydrogenase (GAPDH) using TaqMan® Rodent GAPDH Control Reagents (Applied Biosystems Japan Ltd.).

2.6. Immunohistochemistry

To evaluate the immunohistochemical distribution of molecules identified by microarray analysis, the brains of male pups obtained at PND 20 were fixed in Bouin's solution at room temperature overnight. Ten animals for each group were used except for the untreated control group with six animals.

Antibodies against vimentin (mouse monoclonal antibody, 1:200; Millipore Corporation, Billerica, MA), glial fibrillary acidic protein (GFAP, rabbit polyclonal antibody, 1:500; Dako, Glostrup, Denmark), Ret (rabbit polyclonal antibody, 1:50; Santa Cruz Biotechnology, Inc., Santa Cruz, CA), DCC (mouse monoclonal antibody, 1:40; Leica Microsystems GmbH), and oligodendrocyte specific protein (OSP, same as Cld11, rabbit polyclonal antibody, 1:200; Novus Biologicals, Inc., Co., Littleton, CO) were used for immunohistochemistry. For antigen retrieval, sections were heated in 10 mM citrate buffer in a microwave for 10 min before incubation with anti-vimentin and -DCC antibodies. Immunodetection was carried out using a VECTASTAIN® Elite ABC kit (Vector Laboratories Inc., Burlingame, CA) with 3,3′-diaminobenzidine/H_2O_2 for the chromogen as described elsewhere [13,14]. Sections were then counterstained with hematoxylin and coverslipped for microscopic examination.

Please cite this article in press as: Fujimoto H, et al. Increased cellular distribution of vimentin and Ret in the cingulum induced by developmental hypothyroidism in rat offspring maternally exposed to anti-thyroid agents. Reprod Toxicol (2012), http://dx.doi.org/10.1016/j.reprotox.2012.03.005

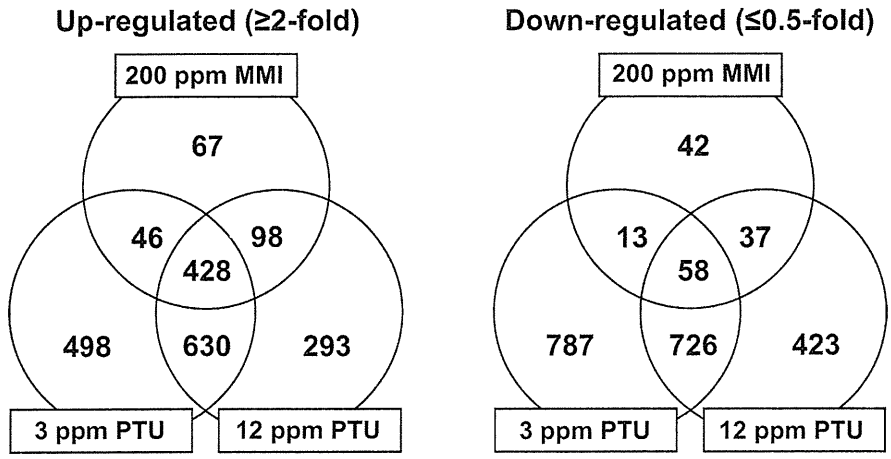

Fig. 2. Venn diagram of genes with altered expression in microarray analysis in response to maternal exposure to anti-thyroid agents. (Left) Up-regulated genes (≥2-fold). (Right) Down-regulated genes (≤0.5-fold).

2.7. Morphometry of immunolocalized cells

The number of immunoreactive cells was quantitatively measured by vimentin and Ret expression in white matter at the cingulum of the bilateral sides using two sections with an approximately 100 μm interval (i.e. four images per animal; Fig. 1), and values were normalized and expressed as those in the unit area (cm^2). GFAP-immunoreactive cells were similarly measured. For quantitative measurement of each immunoreactive cellular component containing vimentin, Ret and GFAP, digital photomicrographs at 100-fold magnification were taken using a BX51 microscope (Olympus Optical Co., Ltd., Tokyo, Japan) attached to a DP70 Digital Camera System (Olympus Optical Co.), and quantitative measurements were performed using WinROOF image analysis software 5.7 (Mitani Corp., Fukui, Japan). To evaluate immunoreactivity of DCC and Cld11 in white matter, staining intensity was scored as 0 (none), 1 (minimal), 2 (slight), 3 (moderate) and 4 (strong) by observation at 40-fold magnification.

2.8. Statistical analysis

Numerical data were assessed by one-way analysis of variance or the Kruskal–Wallis test following Bartlett's test. Statistically significant differences were analyzed by Dunnett's multiple test for comparison with that of the untreated control group. For grading immunohistochemical findings, scores of DCC and Cld11 expression were analyzed with the Mann-Whitney's *U*-test between the untreated control group and each anti-thyroid agent treated group.

3. Results

3.1. Global gene expression analysis

Fig. 2 shows the Venn diagram of genes with altered expression in microdissected cerebral white matter in treated groups in combination or individually in each treated group. Numerous common genes were found to be up- or down-regulated in two of the three treatment groups. The number of genes with up- or down-regulation in response to 3 ppm PTU was higher compared with that of 12 ppm PTU. The number of genes with

Table 1
List of representative genes associated with brain development showing up- or down-regulation common to treatments with MMI and PTU at both 3 and 12 ppm (≥2-fold, ≤0.5-fold).

Accession no.	Gene title	Symbol	MMI	PTU, 3 ppm	PTU, 12 ppm
Up-regulated (20 genes)					
NM_052803	ATPase, Cu++ transporting, alpha polypeptide	*Atp7a*	5.02	11.39	11.09
NM_001108322	T-box 1	*Tbx1*	4.20	4.34	2.31
NM_001191609	Laminin, alpha 5	*Lama5*	4.11	11.57	9.35
NM_031550	Cyclin-dependent kinase inhibitor 2A	*Cdkn2a*	3.59	2.70	3.37
NM_001114330	Glutamate receptor, metabotropic 1	*Grm1*	3.45	2.92	5.89
(NM_001114330)			(3.01)	(2.85)	(2.88)
NM_023091	gamma-Aminobutyric acid A receptor, epsilon	*Gabre*	3.20	3.91	7.46
NM_001107692	Ephrin A4	*Efna4*	3.13	5.07	6.72
NM_001002805	Complement component 4a	*C4a*	3.04	7.15	6.43
NM_019328	Nuclear receptor subfamily 4, group A, member 2	*Nr4a2*	2.97	2.87	4.92
NM_001110099	Ret proto-oncogene	*Ret*	2.89	5.01	4.39
NM_053629	Follistatin-like 3	*Fstl3*	2.85	4.28	6.08
NM_053708	Gastrulation brain homeobox 2	*Gbx2*	2.82	4.73	4.09
NM_019236	Hairy and enhancer of split 2	*Hes2*	2.76	2.93	3.11
NM_001109223	Wingless-related MMTV integration site 16	*Wnt16*	2.71	2.42	3.82
XM_001077495	Nuclear receptor co-repressor 1	*Ncor1*	2.67	2.01	2.97
NM_001012220	Cation channel, sperm associated 2	*Catsper2*	2.54	6.69	4.56
NM_001024275	Ras association (RalGDS/AF-6) domain family 4	*Rassf4*	2.31	4.67	5.43
NM_138900	Complement component 1, s subcomponent	*C1s*	2.12	3.31	3.88
NM_031140	Vimentin	*Vim*	2.11	6.01	4.27
NM_053555	Vesicle-associated membrane protein 5	*Vamp5*	2.04	2.62	3.41
Down-regulated (4 genes)					
NM_013107	Bone morphogenetic protein 6	*Bmp6*	0.23	0.38	0.25
NM_053759	Sine oculis homeobox homolog 1	*Six1*	0.45	0.35	0.46
NM_019280	Gap junction membrane channel protein alpha 5	*Gja5*	0.46	0.16	0.28
NM_133293	GATA binding protein 3	*Gata3*	0.47	0.47	0.24

Abbreviations: MMI, 2-mercapto-1-methylimidazole; PTU, 6-propyl-2-thiouracil.

Please cite this article in press as: Fujimoto H, et al. Increased cellular distribution of vimentin and Ret in the cingulum induced by developmental hypothyroidism in rat offspring maternally exposed to anti-thyroid agents. Reprod Toxicol (2012), http://dx.doi.org/10.1016/j.reprotox.2012.03.005